CHALMERS

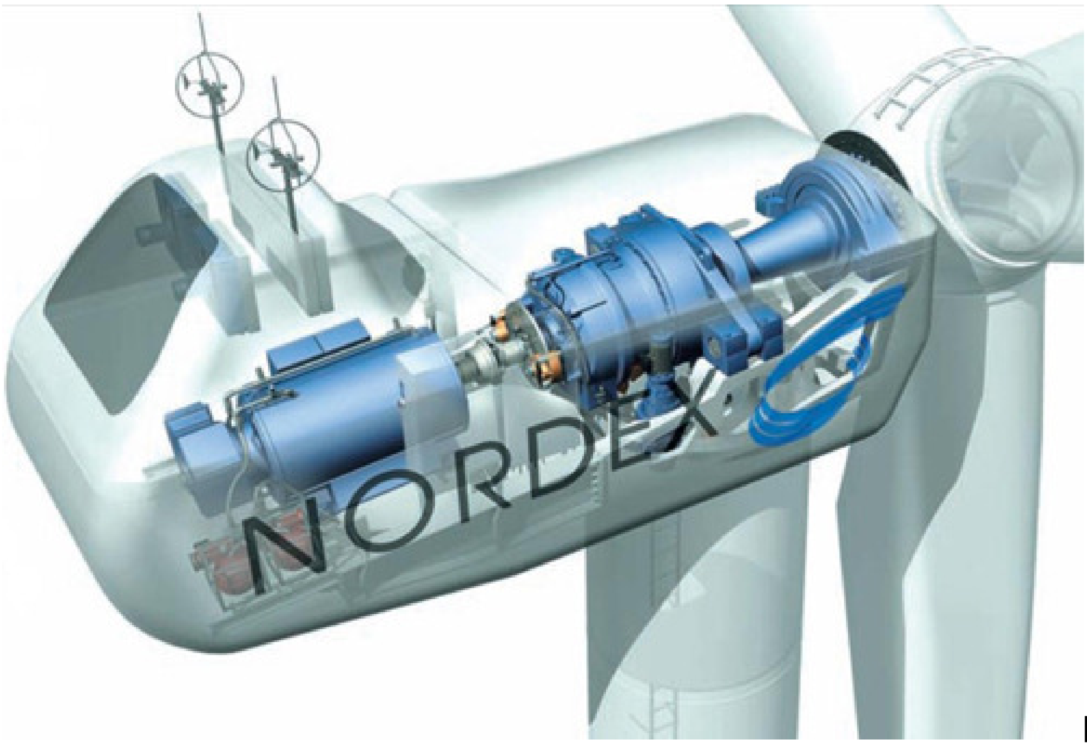

[1]

Modeling of Dynamics of Driveline of Wind Stations: Implementation in LMS Imagine AMESim Software

Master's Thesis in the International Master's programme Automotive Engineering

BINCHENG JIANG

Department of Applied Mechanics
Division of Dynamics
CHALMERS UNIVERSITY OF TECHNOLOGY
Göteborg, Sweden 2010
Master's Thesis 2010:38

MASTER’S THESIS 2010:38

Modeling of Dynamics of Driveline of Wind Stations:

Implementation in LMS Imagine AMESim Software

Master’s Thesis in the International Master’s programme Automotive Engineering

BINCHENG JIANG

Department of Applied Mechanics
Division of Dynamics
CHALMERS UNIVERSITY OF TECHNOLOGY

Göteborg, Sweden 2010

Modeling of Dynamics of Driveline of Wind Stations: Implementation in LMS Imagine AMESim Software
Master's Thesis in the International Master's programme Automotive Engineering

BINCHENG JIANG

Master's Thesis 2010:38
ISSN 1652-8557

Department of Applied Mechanics
Division of Dynamics
Chalmers University of Technology
SE-412 96 Göteborg
Sweden
Telephone: + 46 (0)31-772 1000

Cover:
The typical drive train configuration in the wind turbine from the Nordex wind turbine company.

Chalmers Reproservice
Göteborg, Sweden 2010

Modeling of Dynamics of Driveline of Wind Stations: Implementation in LMS Imagine AMESim Software

Master's Thesis in the International Master's programme Automotive Engineering

BINCHENG JIANG

Department of Applied Mechanics

Division of Dynamics

Chalmers University of Technology

ABSTRACT

The wind power area is booming rapidly and enormous of malfunction of wind turbine components emerges in the market. Therefore, it is time to pay attention to the quality of the design process. In the past years, the industry is a dearth of information on just what goes on in the internal workings of a wind turbine, especially for the drivetrain part. Nowadays, there is a high downtime per failure of drivetrain per year among the different components of the wind turbine due to the rigorous load impacting from the rotor hub and the generator or electrical network faults. The thesis work is kind of pre-study of analyzing the dynamic performance of drivetrain in the wind power station. It is a tentative effort to study the dynamic behavior of the gearbox under normal operation and transient load condition in order to be ready to dig out the reasons of the drivetrain misalignments in the future work. The main objective of the present thesis is to develop the 1-D torsional multibody dynamic model of the drivetrain of wind station taking into account excitation from the aerodynamic force and the response from the generator part of the wind turbine. Furthermore, it is of importance to understand the principal concept of modern wind turbine, especially the typical drivetrain configurations; the modeling approaches and how to build the model for the aerodynamic force and generator torque in AMESim, also how analyze the dynamics of drivetrain. The aim is to analyze the torsional dynamics of wind drivetrain, consisting of free response vibration, transient vibration dynamics and the steady state simulation for the calculation of power losses. Linear analysis is applied for the cases of free vibration and transient torsional dynamics, such as eigenfrequencies, mode shapes etc.

Key words: Wind power, drivetrain, torsional, dynamics, modeling

Contents

Preface

This master thesis work is developed for the Master of Science degree is Automotive Engineering, at Chalmers University of Technology, Gothenburg, Sweden. The supervisor and examiner is Professor Viktor Berbyuk.

First, I would especially thank my supervisor Viktor Berbyuk, for the opportunity he gave to me to take this master thesis and his guidance during the thesis work, not only during the project, but also my way to the future. And also thank the colleagues and staff at Applied Mechanics Department.

Last, but not least, I thank my family and friends for their ever-constant support and guidance. Specifically, I would like to acknowledge Yuwen He, who generously provided the spiritual and material support that enabled me to produce this report.

Göteborg , June 2010

Bincheng Jiang

Notations

English variables

a	Axial interference of induction factor
a'	Angular induction factor
c	Coefficients dependent on the characteristic of the wind turbine
c(r)	Blade cord length
C	(i) Damping coefficient of the shaft
C	(ii) Contact damping of gear stages
C_L	Lift airfoil coefficient
$C_P(\lambda, \beta)$	Power efficient of the wind turbine rotor
C_D	Drag airfoil coefficient
C_{gm}	Contact viscous coefficient of gear meshing
C_T	Thrust coefficient or local thrust coefficient
D	Drag force per unit length of blade
E_q	Equivalent Young modulus
f	Grid frequency
$F_b(x)$	Contact force of gear meshing taking into account backlash
lim	Limit penetration to apply the full damping
L	Lift force per unit length of blade
M	(i) Torque transferred through the gear stages
M	(ii) Air gap moment on asynchronous machine
M_k	Breakdown torque of asynchronous machine
$\widetilde{M}_g$	Torque obtained on the generator
n	(i) Rotating speed of gears
n	(ii) Asynchronous machine rotor speed
n_0	Revolution of generator rotor (revolution per second)
n_1	Speed of rotating field or asynchronous speed (revolution per minute)
N	Number of blades
i	Total gear ratio
J	Inertia of rotating components
K	(i) Torsional stiffness of the shaft
K	(ii) Stiffness referring to gear pairs
K_{gm}	Effective stiffness of gear meshing
K_m	Middle contact stiffness of gear meshing

$K_{hertz}(x)$	Hertz stiffness
K(x)	Contact stiffness of gear meshing taking into account Hertz stiffness
p	Number of pairs of poles
P_{mec}	Mechanical power
r	Radius
s	Slip of asynchronous machine
s_k	Breakdown slip of asynchronous machine
R	(i) Radius of wind turbine rotor
R	(ii) Radius of the sphere used to approximate the contact area of the teeth
R_1	Resistance of stator winding or stator resistance
R_2'	Rotor resistance of on phase of an asynchronous machine transformed on the stator side or rotor resistance
tol	Total clearance between gear teeth
T	Torque transferred on the shaft
U	Voltage of generator
V	Free stream air flow velocity
V_{rel}	Relative speed of the wind
x	Deformation of gear meshing
X_1	Stator leakage reactance
X_2'	Rotor leakage reactance,
$X_{1\sigma}$	Stator leakage reactance
$X_{2\sigma}'$	Rotor leakage reactance
X_h	Air gap reactance or magnetizing reactance
Y	Modulus of elasticity
z	Teeth number of gears

Greek variables

α	Angle of attack
β	Pitch angle
ε	Poisson's ratio
θ	Shaft twist angle
$\dot{\theta}$	Rotating speed of rotating components
$\ddot{\theta}$	Rotating acceleration of rotating components
λ	Tip speed ratio
ξ	Damping ratio of mechanical system

ξ_{gm}	Damping ratio of gear meshing
ρ	Air density
σ	Total leakage
$\emptyset$	Inflow angle
ω	Angular velocity of the wind turbine rotor
ω_n	Natural frequency of mechanical system

Abbreviations

CMS	Craig-Bampton component mode synthesis
DFIG	Doubly fed induction generator
DGCS	Drivetrain generator coupling system
DOFs	Degrees of freedom
DTMS	Drivetrain mounting system
FCs	Functional components
FE	Finite element
FFT	Fast Fourier transform
HSS-D1	High speed shaft bearing downwind 1
HSS-D2	High speed shaft bearing downwind 2
HSS-U	High speed shaft bearing upwind
IMS-D	Intermediate shaft bearing downwind
IMS-U	Intermediate shaft bearing upwind
LRS	Lateral rotating system
MBS	Multi body simulation
PID	Proportional integral derivative
PLC1-D	First planet carrier bearing downwind
PLC1-U	First planet carrier bearing upwind
PLC2-D	Second planet carrier bearing downwind
PLC2-U	Second planet carrier bearing upwind
PMG	Permanent magnet generator
RCS	Rotor drivetrain coupling system
SEE	Spectral Emitted Energy
TVS	Torsional vibration system

1 Introduction and Background

In the last 20 years wind turbines have increased in power by a factor of 100, the cost of energy has reduced. Due to the press of the energy crisis and climate change, it heavily requires the renewable energy, which is also clean and economical. Renewable energy is energy which comes from natural resources such as sun, wind and geothermal heat etc. Wind power is one of the most rapidly developing domains. In 2009, wind power is growing at the rate of 30% annually, with a worldwide installed capacity of 157,900 megawatts. The wind power market has expanded dramatically during the past few years and the growing has mainly focused on the area of larger wind turbines development.

Due to the highly rapid development of the wind power industry, the technicians have a limited time to test the newly product design thoroughly before they are manufactured and utilized in the wind power generation. The issue can actually be avoided by means of more advanced simulation environment and detail complete wind turbine model to perform the necessary simulation.

However, there are enormous wind power stations which have already been erected for a couple of years, so some companies proposed a solution for the problem: condition monitoring system. It is installed on the different components of the wind power system, for example, the main shaft, gearbox, bearing etc to detect the conditions of them periodically or continuously. In this way, the maintenance staff could examine the conditions of the wind turbine components. It is necessary to collect the condition data and make the data analysis in order to know the exact status of the unit. Whether it can work well for a long time or it is closed to broken is decided further. However, this method is kind of actively maintaining the components of the wind power. The staff could not do anything until the defection being examined, and it is a bit difficulty in predicting which component needs to be replaced or maintained.

The wind power area is still booming and not completely mature. So it is time to pay attention to the quality of the design process. In the past years, the industry is a dearth of data on just what goes on in the internal workings of a wind turbine, especially for the drivetrain part [2].

1.1 Thesis background

The thesis work is kind of pre-study of analyzing the drivetrain in the wind power station. Nowadays, there is a high downtime per failure of drivetrain per year among the different components of the wind turbine. Misalignment is discovered and considered as one of the main contributors to the failure of the gearbox [3]. There is a hypothesis that one can use the methodology of mechanical dynamic control theory to resolve this problem, for example, adaptive mounting system, active control or passive control method. It is of importance to torsional vibration analysis of the drivetrain.

As discussed before, however, the huge expansion of the wind power has given rise to some problems due to lack of fully test of the new designs. Most of generators as a part of energy conversion system in the wind power are asynchronous generators with wound rotors, which require an input speed of around 1500 rpm. So the gearbox is introduced to gear up the angular speed of the main shaft of the wind power. The intervention of the gearbox raises some problem related to the longest downtime per failure among the whole wind power components [4]. It is evident that the gearbox is critical to the availability of the wind turbine. It is suggested that this is the main reason for the industry's focus on gearbox failures. Similar results have also been obtained in Sweden [3].

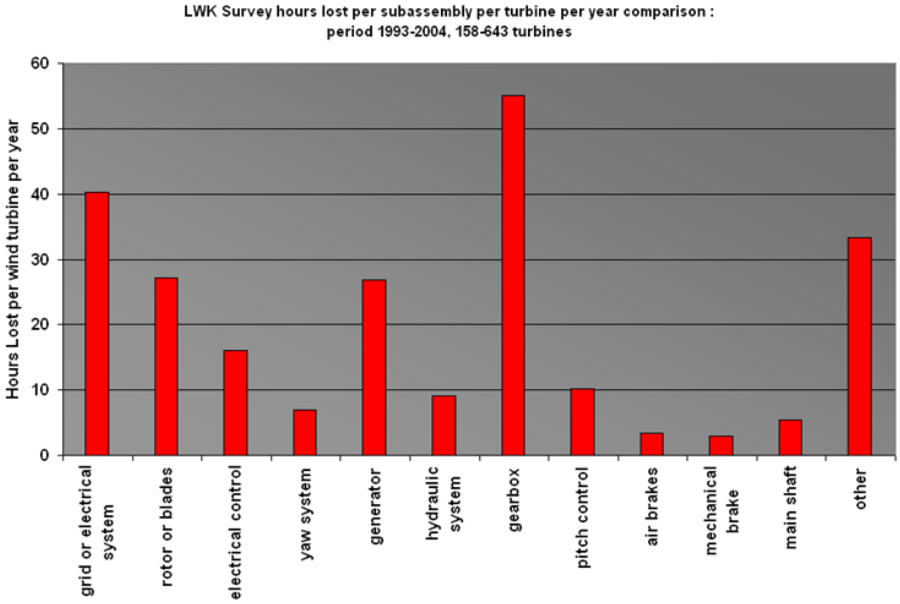

Figure 1.1 Results from LWK surveys assuming a constant failure rate and the HPP model

The reason for the failure is that the first generation of gearboxes was just industrial gearboxes applied in other domains. The conditions under wind turbines operation are quite different. The load impacting on the wind turbine drivetrain varies with the aerodynamic torque on the blades; there are extreme axial, lateral and tilting forces during normal operation due to gusts, power-shifting, start-up and shut-down operation [5, 6]. And these gearboxes are not practical for the wind power station, where needs to withstand large torque transmission and also the rigorous dynamic load caused by some critical cases which are generator or electrical network faults.

The gears and the drivetrain are the components that demand the longest downtime per failure. The reason is that components of the gearbox or drivetrain are always big and cumbersome to disassembly, transport and replace. Sometimes, the spare parts need to be ordered which would prolong the downtime for the overhaul of the gearbox.

Gearbox wear and failure usually result from wear and failure of the primary load carrying elements such as shafts, gears and bearings [7]. Most gearbox failures do not begin as gear failures or gear-tooth design deficiencies [8]. In general, the examined gearbox failures indicate to initiate at several specific bearing locations under certain applications. In some cases it may later deteriorate and propagate into the gear teeth by means of bearing debris and excess clearances which would cause gear teeth surface wear and drivetrain misalignments. Therefore most failures of the gearbox are secondary. Wherein gearbox units are precision instruments: they definitely tolerate little misalignment caused by gravitational loads or fluctuating thrust from the subassemblies. The bearing alignment takes a huge responsibility for the misalignment of the drivetrain, also high precision assemblies.

Whereas the alignment is the key to reduce failure rate of drivetrain, then both downtime and cost of wind power turbine will be diminished, so it is highly significant to analysis the misalignment of the drivetrain. This report is a tentative effort to study the dynamic behavior of the gearbox under normal operation and transient load condition in order to be ready to dig out the reasons of the drivetrain misalignments in the future work.

In order to do analyses regarding to the torsional vibration dynamics of drivetrain in the wind power, one have to build the simulation model then validate it using the field data, some of which can be obtained by existing measurement systems while other required information has not been collected directly. Therefore one should be clear what data is needed to validate the dynamic model of the drivetrain and how many data one can acquire from the condition monitoring system used in some wind turbines for the sake of being as input for developing a condition based maintenance program. The other information data is left unknown and one should put forward a method what kind of sensors are needed and where they can be mounted, etc. This part of validation work is not included in this report.

The master thesis focuses on the analysis of dynamics of wind drivetrain, including free response vibration, transient vibration dynamics and the steady state simulation for the calculation of power losses. Therefore, it is of importance to understand the interface between the drivetrain subsystem and other subsystems in the wind turbine, what it looks like, how they interact with each other.

The wind turbine is divided into four parts: the rotor substructure, the drivetrain substructure, the tower substructure and the electrical substructure. Hence there are three interfaces of wind drivetrain.

1) The interface between the drivetrain and the aerodynamic part is named rotor adaptive system;
2) The interface between the drivetrain and the tower part is called tower adaptive system, more precisely named mounting adaptive system;
3) The interface between the drivetrain and the electrical part is known as generator adaptive system.

At the area of each interface surface, there is the place where the related subsystems transfer torque and force. In general, these forces and torques at the connection points can be composed together into a resultant force and a resultant moment at a certain point of the interface. In this report, the mounting adaptive system is ignored. In future research work, it’s better to take this into account because the supporting system is of importance to the misalignment of the drivetrain in the wind turbine.

1.2 Thesis objective

The main objective of the present thesis is to develop the dynamic model of the drivetrain of wind station taking into account excitation from the aerodynamic force and the response from the generator part of the wind turbine by using LMS Imagine AMESim Software.

The task is to build the 1-D mechanical torsional vibration systems including the rotor blade and the generator components in order to analyze torsional natural frequency and mode shape. The work is intended to be divided into the following parts:

- Description of the principal concept of modern wind turbine, especially the typical drivetrain configurations
- Possible reasons and consequences of misalignments at drivetrain
- Present the methods that how to build the model for the aerodynamic force and generator torque
- Develop computational model of dynamics of drivetrain in wind turbine in AMESim
- Run the computational models built in AMESim and analysis the results, including the free vibration dynamics, transient vibration dynamics and steady state analysis.

1.3 Thesis overview

- Chapter 1- Introduction and background

  This chapter gives an overview and background for this master thesis and also establishes the objective of the present task.

- Chapter 2 - Principle concept of modern wind turbines

  The fundamentals of the components used in a wind turbine are presented. In particular, the typical drivetrain configurations are intended to be reviewed.

- Chapter 3 - Basics of misalignment concept

  Description of the misalignment's basic concept is presented. In this chapter, the causes of misalignment are given and analyze possible misalignments at drivetrain of wind power then point out the specific reasons of misalignment and what will the misalignment results in. The relationship between the misalignments of the rotating machinery and the types of the vibration signatures is covered.

- Chapter 4 - Modeling techniques for drivetrain

  The main work consists of very detailed modeling approaches. The multi-body simulation techniques, used within the scope of the project are to be analyzed. One of these techniques needs to be chosen to build dynamic model for the drivetrain for this report.

- Chapter 5 – Aerodynamic model and generator model

  The Chapter is divided into two main parts: one is that the method how to develop the model for aerodynamic torque at the normal operation; the other is to use the typical $Klo\beta's$ equation for the asynchronous machine.

- Chapter 6 – Models of dynamics of drivetrain

  Construct the mathematical and computational model of drivetrain dynamics of wind turbines by taking into account the torques from the aerodynamics and generator in the AMESim environment.

- Chapter 7 - Analysis of drivetrain in wind turbine

  The focus in this chapter is on analysis of free torsional vibration and transient dynamics of drivetrain. Additional, evaluate the quality performance and power losses of wind turbine due to bearing.

- Chapter 8 - Conclusion and suggestions for future work

  The model developed in this report is 1-D dynamic model, which is the simplest model with one degree of freedom per drivetrain component in order to investigate only torsional vibrations in the drivetrain. In order to take into account the misalignment in the model, it is necessary to introduce more degrees of freedom in the drivetrain and more advanced modeling method for taking into account the misalignment. What's more, the simulation results needs to be verified by measurement data.

2 Principal Concept of Modern Wind Turbine

Wind power is the conversion of wind energy into useful form, such as electricity, by means of wind turbines. A wind energy system transforms the kinematic energy of the wind into mechanical or electrical energy that can be harnessed for practical use. In general, the wind turbine manufacturers usually choose the way that wind electric turbines generate electricity for homes and businesses and for sale to utilities.

Wind turbines can rotate about either a horizontal or vertical axis, the former one called "propeller-style" being more popular; the latter more like "egg-beater". Horizontal-axis wind turbines constitute nearly all of the "utility-scale" turbines in the global market. This report only focuses on the propeller-style wind turbine. In the following content, if mentioning the wind turbines, it represents the horizontal axis wind turbine.

2.1 Drivetrain configurations in wind turbine

This part describes the basic configuration of the most common wind turbines present in the industry nowadays. There are a lot of possible drivetrain configurations for the power transmission depending on the design criteria. On the whole, the drivetrain configurations can be divided into two catalogues: geared drive wind turbine and wind turbine driven without gear stages.

The latter type is also named by direct-drive configuration. This concept supply the possibility to apply the permanent magnet generator (PMG), while the PMG design have many advantages due to its simplicity and potential reduction in size, weight, and cost compared with a wound-field design. However, the gearless configuration requires a full rating power converter at the side of generator output in order to allow the variable speed operation [9]. In addition, the failure intensities of direct drive generator are up to double that of the geared drive generators of similar size. Aggregate failure intensities resulting from generators and converters of direct drive wind turbines are greater than that in the geared drive wind turbines [4]. Therefore, in the wind turbine industry market now, most wind turbine manufacturers are adopting the drivetrain with the gear stages. Wherefore, this report is mainly concentrating on the geared drivetrain.

In Fig 2.1, it demonstrates the typical configuration of the wind turbine with gears. The system components described here are for a common system with the basic features. The name of all the sub-components are the terminology and applicable for almost all wind turbine designs. In particular, the wind turbine consists of the blade, rotor, shafts, gearbox, generator, mechanical brake, pitch system, yaw system, tower etc. In the following content, if mentioning the wind turbines, it represents the geared wind turbine.

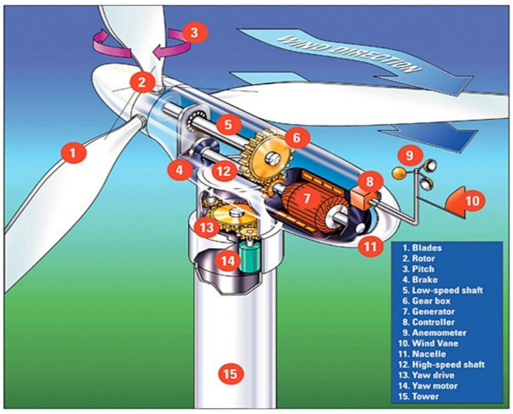

Figure 2.1 Overview of different components of a wind turbine [10]

2.1.1 Description of different structure concepts

The wind turbine with gears may be classified in different ways. Here, one approach is selected: according to the structural configuration outline of wind turbine components. There are three common structure concepts for the wind turbine making up of the modular drivetrain, the partially integrated drivetrain and the integrated drivetrain. Currently, all these configurations are produced by the wind turbine manufacturers and share the wind power market. Hence, there is no general consensus concerning which one has most virtues. There are compared the following layout for three concepts:

- Configuration A−Modular drivetrain configuration: Figure 2.2 shows a widely used standard configuration where all individual components of the drivetrain are mounted onto the bedplate separately.
- Configuration B−Integrated drivetrain: Figure 2.3 represents it comprises the components of the modular type. This compact design is not dependent on the bedplate.
- Configuration C−Partially integrated drivetrain: Figure 2.4 shows that this concept is a combination of the modular and integrated design. It is based on the modular design in that the bedplate is used for mounting the components and some of the substructures are integrated.

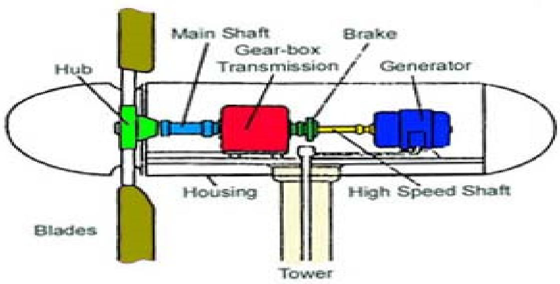

Figure 2.2 Concept A:Modular drivetrain configuration [11]

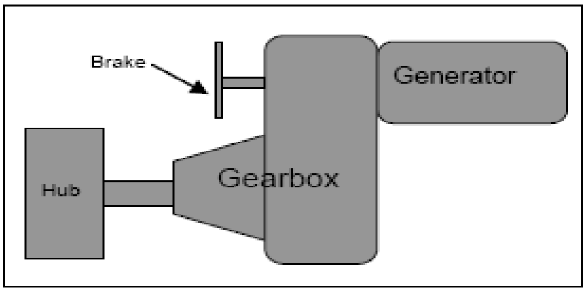

Figure 2.3 Concept B: Integrated drivetrain [12]

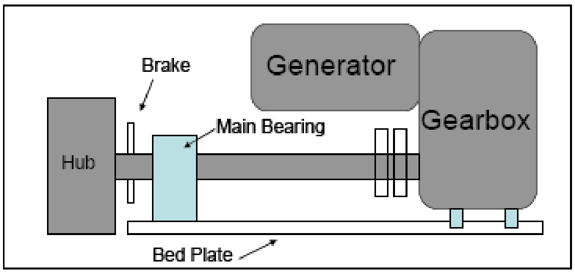

Figure 2.4 Concept C: Partially integrated drivetrain [12]

2.1.2 Comparison of different structure concepts

The modular configuration allows a non-vertical design process, which means that all the components of the drivetrain are supplied by the different vendors. Thus it will consequently reduce the cost dramatically by mean of forming a competitive environment among the suppliers. Regarding to the maintenance cost, the modular wind turbine type is readily to be examined and repaired. The malfunction components are conveniently disassembled from the installed wind turbine and taken place of the new ones. But the main problem is apparent that it is difficult to align the different components from a great number of suppliers. The partially integrated drivetrain has two options: rotor hub gearbox integration and gearbox generator integration. The first one must follow a vertical design process because the gearbox is part of structure in wind turbine. The second one does not require a complete vertical design but it still needs close cooperation between different vendors of gearbox and generators. For the integrated configuration, it is really sensitive to a defective part due to the influence of the entire nacelle, which makes the maintenance cost is extremely a lot. In this concept, the gearbox plays a vital role in supporting the main shaft and also hub. Therefore, the gearbox and bearing housing construction must be robust enough. The integration drivetrain concept has to apply the vertical structure with components suppliers participating in the entire design process closely [13]. The latter two types of wind turbine, due to some parts or fully integrated it is difficult to entirely isolate the drivetrain from the tower and rotor hub. Therefore, the external force or torque from the non-expectation sources are transferred to the mechanical component of drivetrain, leading to the reduction of the component lifetime and increasing probability of aggregate failure intensities.

In a word, the modular concept has most advantages compared with other structured configurations. What is more, in the wind turbine market, currently, most operating turbines follow the modular configuration. Therefore, the report focuses on the modular drivetrain of the wind turbine. In the following content, if mentioning the wind turbines, it represents the modular drivetrain wind turbine.

2.2 Modular drivetrain configurations

A widely used standard configuration, modular drivetrain configuration where all individual components of the drivetrain are mounted onto the bedplate separately is discussed in this section in detail. The various kinds of modular wind turbines are introduced and studied.

2.2.1 Description of different modular concepts

In the modular drivetrain configuration, all individual components are mounted on the bedplate which is structurally connected to the nacelle. This type of construction is divided into three subsets for in-depth study.

- Baseline configuration

The baseline drivetrain, so-called due to its popular commercial applicable concept, employs a multi-stage gear speed increaser. In general, it consists of at least one planetary low-speed front-end followed by two helical or spur parallel gear stages, or one planetary and one helical or spur gear stage in order to obtain the nominal output angular speed suitable for the wound rotor induction generator [9], which is chosen to be the only type of generators.

Whether it needs the partial or full rating power electronics converters depend on the design configuration. For example, a concept available on the market is the 2.0 MW DeWind D8.2. Following the traditional a combined gear stages, the Voith WinDrive Hydrodynamic gearbox is installed. The WinDrive combines a superimposing gear unit with a torque converter. The hydrodynamic torque converter used in the WinDrive decouples the rotor from the generator; therefore it has the capability of dampening vibrations and shocks in the drivetrain. The transmission ratio is controlled, which leads to a wide ratio range. The synchronous generator connects directly to the grid so the power converters are not required [14].

- Gear-driven, low-speed configuration

This concept benefits both from gearing and specific generator. The type of the single gear stage followed by a low to moderate speed generator decreases the size of generator. Either a wound rotor synchronous generator or a permanent magnet generator is employed in this concept.

- Gear-driven, multiple-path configuration

Multiple-path drivetrain configurations can range from multiple low-speed paths where multiple generators are driven by a single-stage gear path to multiple high-speed generators driven by multiple separate gear paths. Permanent generators are the most promising option of the multiple-path design alternatives.

In this report, the baseline is chosen to be analyzed because of its widespread commercial installed base [9]. In the following content, if mentioning the wind turbines, it represents the baseline drivetrain wind turbine.

2.2.2 Description of different baseline configurations

This section describes the two typical gear-driven, modular concepts employed in the wind turbine industry market. Nowadays, the gear stage always consists of three stages which could be several combinations types. While generally the planetary gear is installed at the low-speed shaft rear-end, followed by the two helical or spur parallel gear stages or hybrid gear stages.

The first concept is illustrated in Figure 2.5 below. The main shaft whose front end is connected to the hub by coupling is supported by two separate bearings. The gearbox is held by the shaft with torque restraints.

The drivetrain with main shaft supported by two spherical or cylindrical roller bearings that transmit the side or radial loads directly to the frame by means of the bearing housing, which prevents the gearbox from receiving additional loads, reducing malfunctions and facilitating its maintenance service.

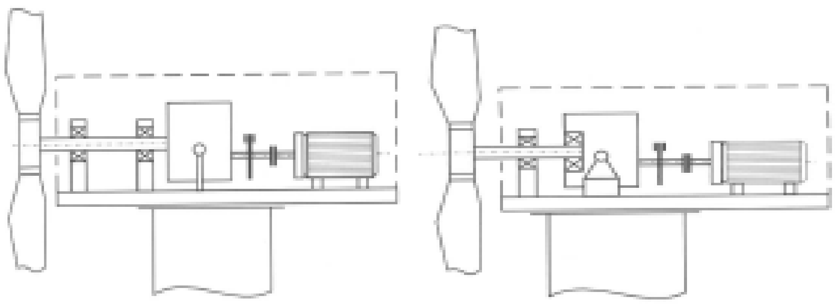

Figure 2.5 Two-point mounting arrangement & Three-point mounting arrangement [15]

The right one of Figure 2.5 demonstrates what the second driveline concept looks like. The rear bearing for the main shaft is integrated into the gearbox. It looks like three point support so it is called three-point suspension. However, indeed this configuration has four support points; hence in some paper this is called 'four-point mounting' type drivetrain.

The drivetrain is supported at three points immediately above the top flange of the tower. The rotor loads are transferred from the rotor shaft to the main frame via the three-point bearings. The rotor-side self-aligning roller bearing is directly mounted on the main frame as a fixed bearing. The movable bearing is integrated into the gearbox, connecting to the main shaft via a shrink disk or flange. The bearing loads acted by the gearbox are transferred to the main frame via an elastically mounted torque-bearing suspension [16].

2.3 Conclusion

To sum up, in this chapter, there is a brief outline of the wind turbine existing in the turbine market. Also for each drivetrain configuration, their own features are presented concisely and investigated, then make a trade-off among the different mechanical layout. Finally, the most widespread and industry-standard drivetrain configuration in each category is selected. In following sections, the wind turbine mentioned stands for the modular baseline wind turbine with multi-stage gears, including the wound rotor asynchronous generator.

3 Basics of Misalignment Concept

Misalignment is a potential largest reason for the failure of the drivetrain. While this leads to the longest downtime compared with other wind turbine failure components repair, it is critical that to understand the basic knowledge of misalignment, especially the aspects of the causes of the misalignment, consequences of the misalignment, and how to detect the rotary machinery misalignment.

3.1 Introduction to shaft misalignment

Shaft misalignment is the leading cause of machine failure, resulting in premature component wear, system breakdowns, production downtime and expensive repairs.

Misalignment is a condition where the centerlines of coupled shafts do not coincide. It is the deviation of relative shaft position from a collinear axis of rotation [17] Shaft misalignment can occur in two basic ways: parallel and angular as shown in Figure 3.1. Actual field conditions usually have a combination of both parallel and angular misalignment so measuring the relationship of the shafts gets to be complicated.

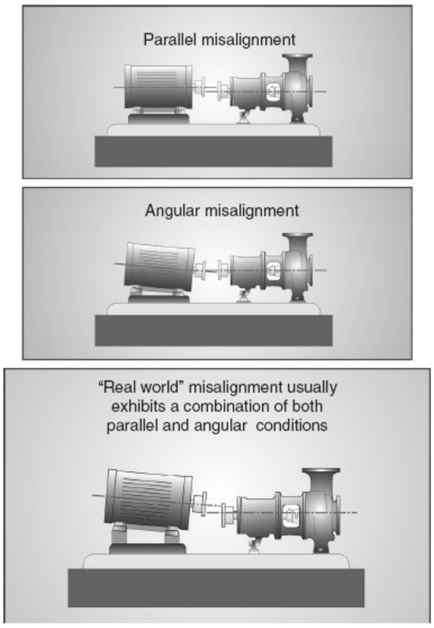

Figure 3.1 Misalignment types [18]

3.2 Types of misalignment

3.2.1 Parallel misalignment

If the misaligned shaft centrelines are parallel but not coincident, this kind of misalignment is named parallel misalignment. It is also known as offset misalignment. If angular speed varies with time, the imbalance vibration varies as the square of the speed, but misalignment-induced vibration will not change in level. This is typically measured at the coupling center [17]. Figure 3.2 is a typical demonstration of parallel misalignment.

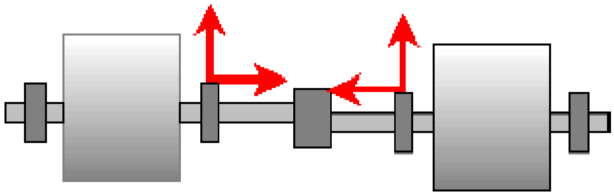

Figure 3.2 Parallel misalignment [17]

3.2.2 Angular misalignment

If the misaligned shafts meet at a point but not parallel, this type of misalignment is named angular misalignment. It is the difference in the slope of one shaft, usually the moveable machine, as compared to the slope of the shaft of the other machine, usually the stationary machine. Angular misalignment always generates a strong vibration at 1× rotational speed and some vibration at 2× rotating speed in the axial direction at both bearing, and of the opposite phase [17].

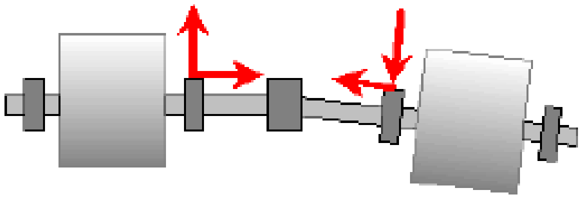

Figure 3.3 Angular misalignment [17]

3.2.3 Mixed misalignment

In reality, most cases of misalignment are a combination of the two above described types, and diagnosis is based on stronger 2× rotating speed peaks than 1× rotational speed peaks and the existence of 1× rotational speed and 2× rotating speed axial peaks [17].

The best alignment of any machine will always occur at only one operating temperature, and it should be its normal operating temperature. In other words, the misalignment varies with the change of temperature. This is a vital factor for one consideration before assembly. In the operation, the internal temperature of the rotating machine will increase dramatically due to friction and thermal effect. It is imperative that the vibration measurements for misalignment diagnosis be made with the machine at normal operating temperature [18].

3.3 Reasons of misalignment

In wind turbine, misalignment could occur at coupling connections between two shafts and bearing locations. There is not only one source responsible for all the misalignment of drivetrain in wind turbine. In general, a couple of reasons will be considered to be contributed misalignment result. Misalignment is typically caused by the following conditions [17]:

- Inaccurate assembly of components, such as gearbox, bearings, etc

- Relative position of components shifting after assembly
- Distortion of flexible supports due to torque, especially in the case of transient condition due to gusts, short circuit etc.
- Temperature induced growth of machine structure during the operation of components
- Coupling face not perpendicular to the shaft axis
- Soft foot, where the machine shifts when hold down bolt are torque
- The naturally occurring curvature of center mounted or overhung shafts. For the shafts in wind turbine, whether this influence is ignored or not needs to be verified further.

In addition these elements, there are also three factors that affect alignment of rotating machinery: the speed of the drivetrain, the load condition transmitted in drivetrain, the maximum deviation and distance between the flexing points or points of power transmission [18].

3.4 Detecting misalignment on rotating machine

In order to eliminate the severity of misalignment in wind turbine, it is better to be able to be sure the state of the misalignment. Misalignment in the drivetrain of wind turbine can cause vibrations that reduce the service life and availability of gears. These errors can be identified by means of vibration analysis through condition monitoring systems.

3.4.1 Vibration analysis techniques

The Vibration Signature of a machine is the characteristic pattern of vibrations that the machine produces when it is in normal operation. Vibration information is typically displayed in two different ways: in the time domain and in the frequency (spectral) domain. The data for vibration analysis is coming from the condition monitoring systems.

- Time-domain: Time domain signals of vibration level in the machine are used in the early stages of vibration analysis when analog instruments are mainly adopted and the technology, i.e. fast Fourier transform (FFT), microprocessors not available [19].
- Frequency Domain: Fast Fourier Transform is the most common way to transform signals into the frequency domain. The advantage of frequency domain analysis over time domain analysis is its ability to easily identify and isolate certain frequency component of interest. With the use of an FFT signal analyzer, vibration signatures can be taken that split the complex overall vibration signal and enable one to look at various frequencies of the sensor output [18, 19]

3.4.2 Condition monitoring services

Condition Monitoring is a machine maintenance tool which is becoming a component of long-term service packages. Nowadays, it is widespread in wind turbine industry because of the reduced costly unscheduled machine down time. It has the power to eliminate breakdowns, reduce maintenance costs, increase production and operational capacity. Condition-based maintenance for offshore wind turbines will improve reliability and increase the availability and hence the cash return for operators [20].

Even the most thorough and comprehensive routine maintenance program cannot stop faults developing in machinery. The worst-case scenario is that faults lead to unexpected failures before next scheduled maintenance break. Condition Monitoring puts one in the driving seat to actively prevent breakdowns and optimize maintenance resources where and when they're needed. Condition Monitoring assess the health of a machine by periodic or continuously monitoring and analysis of data obtained during operation. Condition Monitoring is an efficient and non-intrusive to the production process and with the proven potential to save thousands of pounds in secondary damage, lost production and unnecessary maintenance. It is proven that preventative maintenance approach for early fault detection and prevention in all types of production machinery.

The SKF WindCon 3.0 online condition monitoring system enables maintenance decisions to be based on actual machine conditions rather than arbitrary maintenance schedules. It has the ability to monitor on an unlimited number of turbines and turbine data points. Sensors and software combine to continuously monitor and track several operating conditions: misalignment, mechanical looseness, foundation weakness, gear damage, resonance problems, etc[21].

Using vibration sensors mounted on a turbine's main shaft bearings, drivetrain gearbox, and generator, as well as access to the turbine control system, the system collects, analyzes, and compiles a range of operating data. Therefore, the system is a combination of condition monitoring system and vibration analysis tool.

The type of sensors used depends more or less on the frequency range, relevant for the monitoring:

- Position transducers for the low frequency range
- Velocity sensors in the middle frequency area
- Accelerometers in the high frequency range
- Spectral Emitted Energy (SEE) sensors for very high frequencies (acoustic vibrations)

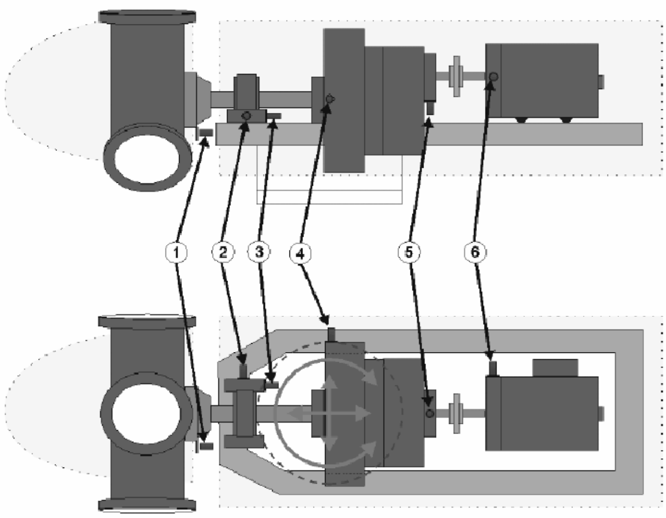

Figure 3.4 Sensor configurations in the drivetrain [22]

4 Modeling Techniques for Drivetrain

4.1 Introduction

Accurate analysis of the drivetrain demands sufficient load data and detail dynamic behavior of the drivetrain. Therefore, a structural model approach is required to develop drivetrain model in order to describe all motions and deformations in the system. In combination with inertia and stiffness damping properties of all drivetrain components, the suitable structural model is capability of supplying insight in the overall dynamic behavior of a drivetrain. There are various ways to classify the modeling approaches for the drivetrain. Here, according to the level of modeling complexity for the drivetrain, three modeling methods are in use in the industry: the rigid multibody simulation (MBS), the finite element (FE) simulation and the flexible MBS technique [23].

4.2 Possible mathematical approaches

4.2.1 Rigid multibody simulation

A simulation model of a complete drivetrain is usually based on a rigid multibody formulation. In this way the drivetrain is divided into discrete rigid bodies, which yields typically a relatively small number of degrees of freedom (DOFs). The joints between the non-deformable bodies introduce the flexibility and damping for the model.

The main advantage of a rigid MBS analysis is to study the overall motion of the drivetrain components, rather than their deformation due to dynamic force. This motion corresponds to the DOFs of a body. In general, before the analysis of internal stress and strain of the drivetrain, it is better to start with the investigation of the drivetrain torque in order to further studying the dynamic drivetrain loads. Therefore, at least one DOF of individual bodies in a drivetrain is required. This type multibody model in which the DOFs per body are limited to one torsional DOF only, is further called purely torsional multibody model [23].

Six DOFs model can be seen as an extension of purely torsional multibody models: instead of just one (torsional) degree of freedom, all bodies have six DOFs. All bodies are still assumed to be rigid, but due to their six DOFs, more accurate and complicated dynamic behavior of components can be provided. Therefore the coupling between two bodies has twelve DOFs, which is always a spring-damper system. It represents force-displacement relationships between two components, leading to introduce flexibilities into the system. Frequently, it will facilitate a more detailed description of gear mesh, bearing stiffness, where the additional flexibility is situated [24-26]. For the sake of simplicity, linear springs are used to model the bearing and gear mesh stiffness [23].

The extension from a torsional vibration model to a rigid multibody model adds the possibility to investigate the influence of gear meshing and bearing flexibilities on the internal dynamic performance of the drivetrain, without the complicated calculation of the stiffness reduction factors during the development of the model. All drivetrain components are still treated as rigid bodies, but now have a full set of six DOFs instead of only one of the purely torsional multibody model, which implies that besides only torsional modes, other non-torsional eigenmodes on the gearbox dynamics are presented. In addition, the gearbox housing, bearing housing, such as the rather flexible components cannot be simply included in torsional multibody mode due to the behavior of these components are too complex to be modeled using only one DOF [24].

4.2.2 Finite element simulation

The FE analysis is the most detailed modeling technical approach used in the internal stress or loads analysis of individual components in the system. In general, it is employed to discrete the flexible components into a large number of DOFs in the order of magnitude of 10,000 up to 1,000,000. It leads to the relatively slow calculation with respect to time domain and high requirement of computer CPU for a large complex system [23].

In reality, the mass and inertia properties of individual component are distributed to the nodes, which include the flexibility of the component. Each element has the maximum six DOFs and a complete FE model could achieve a large number of elements in order to take into account the deformation of the drivetrain components. Consequently, the FE models yield detailed information about the internal stress and strain. Therefore, in case of a drivetrain, the use of FE models is generally limited to the analysis of an individual drivetrain component while not the whole wind turbine system. Normally, the FE approach is typically applied in the critical drivetrain components, such as the bearing, gear teeth etc.

4.2.3 Flexible MBS technique

The rigid MBS simulation as discussed in Section 4.2.1 considers that each body is not deformable. But this assumption is not valid especially when the behaviors of the adjacent components influence each other, For example, it cannot be assumed as rigid when a drivetrain component has an eigenfrequency closed to a frequency response of the system. In addition, the flexibility of the individual body is not taken into consideration resulting in lack of information referring to the internal stress and strain of components. However, the FE simulation seen in Section 4.2.2 has sufficient information for the analysis of dynamics of drivetrain at the cost of the long time calculation for the drivetrain of wind turbine. This problem can be solved by a flexible MBS technique.

This method is based on the rigid MBS while additional FE models of the component are reduced to its modal representation, which includes usually its static deformation and its dynamic response properties [23]. The approach combines the advantages derived from both MBS model and FE model. Among this kind of model, the MBS model plays a role of representing the system overall behavior due to six DOFs of each body; the FE models are reduced to an extra set of DOFs by means of the Craig-Bampton component mode synthesis (CMS) technique to introduce the internal stress and strain information of some certain components.

It can be considered, on one hand, as an extension of the MBS model with the purpose of simulating more details or, on the other hand, as a reduction of the FE analysis in order to reduce the computational time. The MBS added value of this technique has the ability to demonstrate the modal influence of the flexibilities interconnecting the rigid components. The FE main advantage is the possibility of describing local component flexibilities and the evolution of the dynamic stress in the drivetrain continuously with regard to time [24].

A more realistic and accurate representation of model is obtained if introducing the flexibility of components as a material property. Therefore, the means would supply with sufficient dynamic information of the drivetrain model, not only for the individual components also for the whole behavior of the system. There are three objectives using flexible MBS technique:

- A detailed description of the drivetrain including the internal deformation produce more accurate dynamic behavior
- A more realistic description of a body's static flexibility and of its dynamic behavior yields a more accurate simulation results of component loads
- The simulation of internal deformation can be transferred into local stresses and strains, which are required in fatigue calculations and prediction of life time of critical components.

4.3 Description of interesting approaches

The multibody simulation technique is well-established method to analyze not only the torsional behavior of the overall drivetrain but also the detail loads for internal individual components. In this report, the torsional rigid multibody simulation approach is selected to apply in the modeling of dynamics of driveline in the wind turbine as an initial research step. The concentration is put on the torque transferred in the drivetrain and eigenvalues for the torsional model.

4.3.1 Purely torsional multibody models

During the early design stage of the drivetrain, modeling the internal dynamics of a drivetrain is only focusing on torsional vibrations. This torsional modeling approach gives a valuable first insight in possible torsional eigenfrequencies and mode shapes. In the light of simulation results, a first estimate can be made of the effect of early design changes to individual components on overall drivetrain dynamics.

This approach accounts for the torsional compliances resulting from the bending and contact deflection of the gear teeth, as well as torsional deflections of the shafts. The model ignore the added torsional compliance from bending of shafts and from bearing deflection [27]. Spring dampers joining both gears are used to simulate gear interaction. These joint forces lie along the action line and the gear teeth are subjected to the tangential forces [25]. The overall torsional response of the system is obtained, as well as the response from the internal components in a dynamic manner. The shaft is simulated by torsional spring dampers, giving the insight of the torsional shaft deflection as a separate parameter. All the respective torsional inertias from each individual component have to be calculated from the mass and geometries as inputs for the models [28].

In a torsional multibody model, each rotating body has exactly one DOF, while the five other DOFs are fixed, so the equations of motion would not include them and hence the coupling connection of two bodies involves only two DOFs. Only the torsional inertia is required as input for the drivetrain component; additionally, the torsional stiffness damping of the rotating shafts and the gear mesh stiffness are the only flexibilities represented in a direct way at Stage 1 that is discussed in Section 6.3.2, while the model of Stage 2 would take into account the backlash influence in the gear contacting. The torsional stiffness of a shaft (K_{shaft}) between two bodies is included in the equations of torque as shown in following equation [25].

$$T = K_{shaft}\,(\theta_2 - \theta_1)$$

The torsional MBS is able to determine both torsional eigenfrequencies as well as excitation frequencies of shafts, gear meshing. Furthermore, possible resonances can be detected from the simulation results and visualized by way of a Campbell diagram [24].

Only torsional modes can be analyzed, since other mode shapes cannot be predicted by means of a torsional multibody model. However, in order to simulate the loads at certain position in the drivetrain, it needs to be done by post-processing of simulation results. In general, under this situation, it requires more detailed model and more accurate analysis techniques, rigid six DOFs MBS approach or flexible MBS formulation.

4.4 Torsional vibration basics

Torsional vibration could be a problem in wind turbine where most of its subsystems are rotating around their own centerlines. There are two types of coupling in the rotary system, which is referred to as “rigid” and “flexible”. Most of the rotating machine, the couplings fall into the rigid definition. However, in reality, all components have some certain degree of flexibility. In some case, the designer introduces the flexible coupling as damping effect or torsional vibration low-pass filter. The flexible one has ability to allow for some certain degrees of misalignment and eliminate part of pulsating torque from the driver, vibration and shock, which lead to reduce the severity of torsional vibration problems [29].

The torsional vibration system (TVS) is always lightly damped, unlike the lateral rotating system (LRS). In this situation, the pure TVS mode easily results in a serious system failure due to the excitation from the pulsating input. While the TVS mode is always uncoupled from the LRS mode, so it can be the routine behavior that the TVS undergoes continuously or intermittently unforeseen high amplitude under the forced system resonance without showing any serious signs of shaking, initial fatigue. Until the shaft or other rotating components are definitely destroyed or premature failure, namely, there is no indication of the failure of the TVS mode. Therefore, it comes to a strong conclusion that the TVS mode is deserved to be a significant designing factor and also be paid attention to study [30].

4.4.1 Free torsional vibration

A natural frequency of a TVS is a frequency at which the inertia and stiffness torques are completely in balance. Owing to lack of damping, if the excitation acts at the natural frequency, the vibration response of the TVS is infinite amplitude which is a worst case for the mechanical vibration system. When the TVS are at a steady-state mode under the specific frequency, the deflection of the system exhibits a specific pattern called mode shape or eigenvector. This frequency is referred to as the eigenvalue [29, 31].

Free torsional vibration analysis is conducted when the system is simulated without external excitation. Therefore, if there is a non-zero initial condition, the TVS vibrate at the periodic oscillation of torsional motion around the equilibrium position.

Consider a free-body spring-mass of inertia system in which the spring is torsional massless. The spring is elongated from its rest equilibrium point. Assuming that the inertia rotates on a frictional surface, the only force acting on the mass is the spring torque; the motion of the spring is in the linear stage. For this simply system, the mathematical model is [32]:

$$J\ddot{\theta} + K\theta = 0$$

In the situation of lateral vibration, the natural frequency is determined by the stiffness and mass of the system. In the same way for the TVS, the torsional natural frequency is dictated by the torsional stiffness and the mass moment of inertia, as follows:

$$\omega_n = \sqrt{\frac{K}{J}}$$

Where K the torsional stiffness, J the mass moment of inertia and ω_n the torsional free vibration natural frequency (its unit is radians per second). If the natural frequency uses Hertz as its unit, it can be done by the following formula:

$$f = \frac{\omega_n}{2\pi}$$

4.4.2 Free damped torsional vibration

Due to the existence of damping in the TVS, so the vibration oscillation dies out gradually if there is no applied torque. The damper forms the physical model for damping the vibration behavior of the system. The force is proportional to the velocity of motion, in an opposite direction of that of motion. The additional damping factor contributes the motion of the simple spring-inertia system and the equation of motion is modified:

$$\mathrm{J}\ddot{\theta} + \mathrm{C}\dot{\theta} + K\theta = 0$$

Where C the viscous damping coefficient, has unit of $Nm/(rad/s)$.

The values of the mass moment of inertia and the torsional stiffness are readily to obtain by calculation or measurement but it is not straightforward to introduce damping in a drivetrain. Especially determining the absolute value of damping behavior for the components of drivetrain is complex [23].

In order to analyze the free damped vibration system, it is convenient to define the critical damping coefficient, by

$$C_{cr} = 2\sqrt{JK} = 2J\omega_n$$

Furthermore, the nondimensional factor, called damping ratio ξ, which determines the behavior of the system, expressed by the following equation:

$$\xi = \frac{C}{C_{cr}}$$

Therefore, the critical damped vibration system has the damping ratio of 1. If the mechanical vibration system is critically damped, the system returns to the equilibrium point in the least possible time.

4.5 Conclusion

During the whole design process of driveline in wind turbine, simulation techniques are supposed to be able to predict the dynamics of the drivetrain. Multibody system simulation is selected to capture the dynamic behavior. In the first stage, the torsional multibody approach is applied to analyze the torsional vibration in the drivetrain to form the starting point as a validation reference. Then the state-of-the art 6 DOFs rigid MBS with discrete flexibility form the intermediate point to study the whole system motion of dynamics. In a final step, component flexibility is added and the dynamic behavior is compared to the starting reference [28]. The detailed description of the drivetrain would create more realistic behavior of dynamics and more accurate component local loads. The fatigue lifetime of critical components is calculated by the post-processing. In this report, only the torsional MBS is employed in the AMESim. The other two simulation approaches are also necessary if more detailed dynamic information of drivetrain is required.

5 Aerodynamic Model and Generator Model

It is necessary to decompose drivetrain from the whole wind turbine in order to build the dynamic model for the drivetrain and analysis of the dynamic response. The connecting interfaces of the drivetrain consist of three parts, which are all the adaptive systems. The parts that link the rotor and the generator to the drivetrain are represented by the coupling system, which are named individually rotor drivetrain coupling system (RDCS) and drivetrain generator coupling system (DGCS). Drivetrain mounting system (DTMS) is the interface between the drivetrain and the other components to play a role of the main shaft support and the gear box suspension.

Instead of the connecting to the other components, the coupling systems and the mounting systems represent by a resultant force and torque.

Therefore, there are three levels to analyze the dynamic model. First, the input data just includes the force and torque from the RDCS and simulate it to get the output from the DGCS and DTMS. Second, the input data consists of RDCS and DTMS, and obtain DGCS output. Thirdly, the input data comprises the information from RDCS and DTMS, the response from DGCS. The objective of the dynamic model is to analyze the dynamic behavior of the drivetrain. Finally, try to improve the dynamic behavior and the performance of the drivetrain by means of modifying the coupling systems and the mounting systems.

In this report, so as to make the dynamic model of drivetrain reasonable and accurate, it is of importance to take into account the interaction between the rotor blade and the drivetrain, the drivetrain and the generator. Due to the torsional vibration model only concentrate on the rotation behavior, so DTMS is ignored in this report, though it can eliminate the severity of misalignment in theory. RDCS and DGCS are represented by the resultant torques that comes from the aerodynamic and generator models. Therefore, the approaches to develop the models for the aerodynamic and electromagnetic torques are demonstrated following.

5.1 Turbine rotor aerodynamic models

A wind turbine is a device for extracting kinetic energy from the wind. The power production from the wind counts on the interaction between the rotor and the wind. Practical horizontal axis wind turbine designs use airfoils to transform the kinetic energy in the wind into useful mechanical energy which can be transformed into the electricity [33, 34].

Different approaches can be used to calculate the aerodynamic torque acting on the rotor hub. The most advanced one is based on the blade element momentum theory [33-35]. This method refers to an analysis of forces at a section of the blade, as a function of blade geometry. There are two other ways to calculate the power coefficient firstly, then to obtain the mechanical power.

5.1.1 Blade element momentum theory

The method gives good accuracy with respect to time cost. In this method, the turbine blades are divided into a number of independent elements along the length of the blade. At each section, a force balance is applied composing lift and drag with the thrust and torque produced by the section. Meanwhile, the axial and angular momentum is also balanced. It can produce a series of non-linear equations which can be solved numerically for each blade section [33-36].

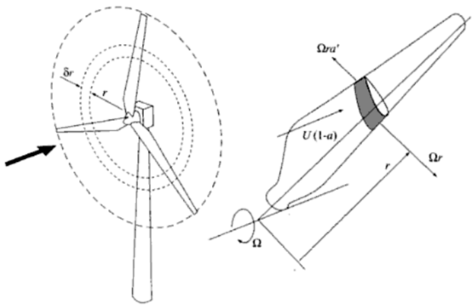

Figure 5.1 A blade element sweeps out an annular ring [34]

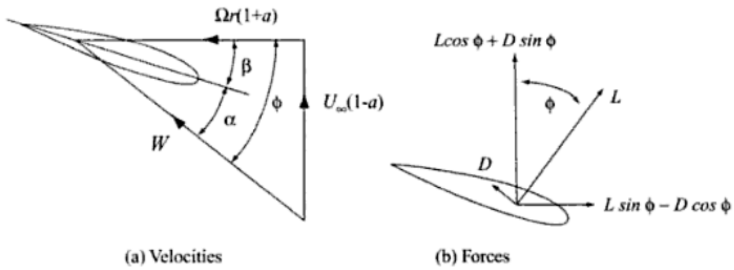

Figure 5.2 Blade element velocities and forces [34]

The lift force L per unit length is perpendicular to the relative speed V_{rel} of the wind:

$$L = \frac{\rho c(r)}{2} V_{rel}^2 C_L \tag{5.1}$$

Where *c(r)* is the blade cord length, the drag force *D* per unit length, which is parallel to V_{rel} is:

$$D = \frac{\rho c(r)}{2} V_{rel}^2 C_D \tag{5.2}$$

Since only the forces normal to and tangential to the rotor-plane are of interest, the lift and drag forces are projected on these directions, Figure 5.2.

$$F_N = L\, cos\emptyset + D sin\emptyset \tag{5.3}$$

And

$$F_T = L\, sin\emptyset - D cos\emptyset \tag{5.4}$$

Where $\emptyset$ the inflow angle.

The lift and drag airfoil coefficients C_L and C_D are generally given as functions of the angle of attack,

$$\alpha = \emptyset - \beta \tag{5.5}$$

Where $\emptyset$ is the inflow angle, β is the pitch angle and α is the angle of attack

Further, the inflow angle is:

$$tan\, \emptyset = \frac{(1-a)V}{(1+a')\omega r}$$

If α exceeds about 15º, the blade will stall. This means that the boundary layer on the upper surface becomes turbulent, which will result in a radical increase of drag and a decrease of lift.

The lift and drag coefficients need to be projected onto the normal and tangential directions.

$$C_N = C_L cos\emptyset + CD\, sin\emptyset \tag{5.6}$$

And

$$C_T = C_L sin\emptyset - C_D cos\emptyset \tag{5.7}$$

The torque on the control volume of thickness dr, is since F_T is force per length

$$dT_{aero} = rNF_T dr = \frac{\rho N}{2} \frac{V(1-a)\omega r^2(1+a')}{sin\emptyset\ cos\emptyset} cC_T dr$$

Where *N* denotes the number of blades.

5.1.2 Analytical approximation

The relation between mechanical power input and wind speed passing the rotor plane can be written as follows [33, 34, 37]:

$$P_{mec} = 1/2\rho V^3 \pi R^2 C_P(\lambda, \beta) \tag{5.8}$$

where P_{mec} is the mechanical power input, ρ is the air density, V is the wind speed, R is the rotor blade radius and C_P is the power efficient of the wind turbine rotor which is a function of pitch angle β and tip speed ratio λ. The tip speed ratio is obtained from $\lambda = (\omega R)/V$

$C_P(\lambda, \beta)$ characteristic of a turbine aerodynamic model can also be approximated by a non-linear function. One such function is given by [38] in the following form

$$C_P(\lambda, \beta) = c_1(c_2 - c_3\beta - c_4\beta^x - c_5)e^{-c_6} + c_7\lambda \tag{5.9}$$

Coefficients $c_1\ to\ c_7$ are dependent on the characteristic of the wind turbine in question; the following are exemplary values for $c_1\ to\ c_7$ as given in [38]:

$$c_1 = 0.5, c_2 = \frac{116}{\lambda_i}, c_3 = 0.4, c_4 = 0$$

$$c_5 = 5, c_6 = \frac{21}{\lambda_i}, c_7 = 0.0068, x = 1.5$$

Where

$$\lambda_i = \left(\frac{1}{\lambda + 0.08\beta} - \frac{0.035}{\beta^3 + 1}\right)^{-1}$$

In this report, the wind speed is set in the range of speed where the rated power occurs, so the pitch angle vary a bit around one certain angle. Since the wind speed is around nominal speed the rotating speed of the main shaft is also in the small range around the rotor nominal revolution. The determination of the desired pitch angle is by means of proportional integral derivative (PID) control theory. The input is the difference of the nominal angular speed and the actual rotating speed of the main shaft. The application in AMESim is shown in the following figure.

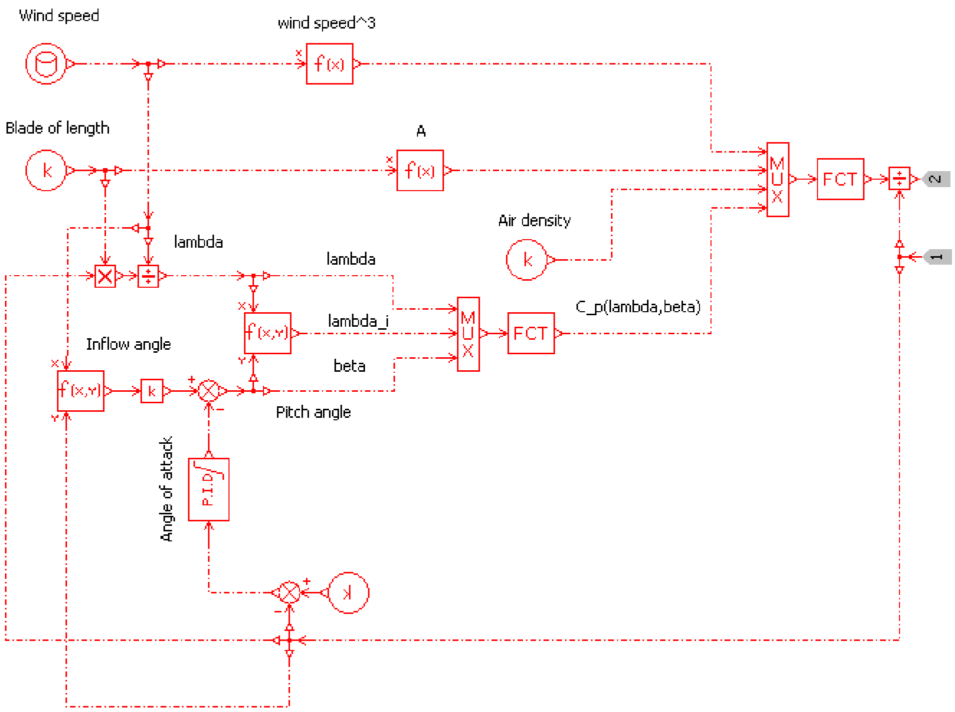

Figure 5.3 Aerodynamic torque representations

The port 1 in the diagram is the feedback of low-speed shaft revolution and the output of the model is port 2 whose value is the mechanical torque obtained from the wind.

There is another way to obtain the power coefficient. This model is suitable for long-term drivetrain system studies where the dynamics of the aerodynamic system can be ignored without neglecting the influence of wind speed fluctuation on mechanical output power.

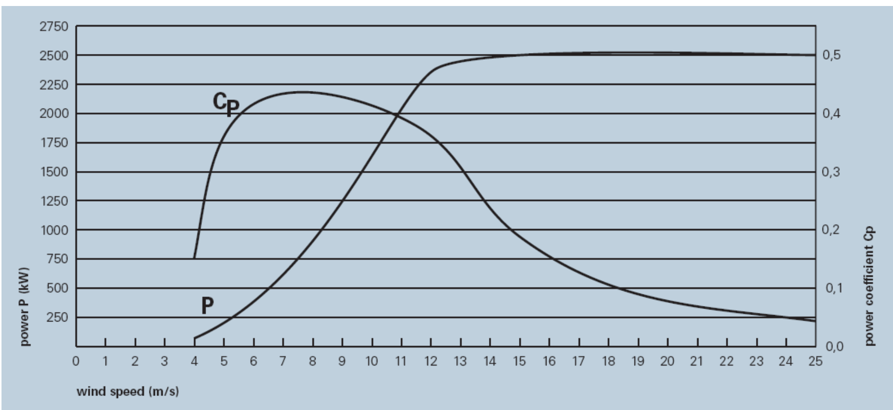

Figure 5.4 Power coefficient and power production as a function of wind speed for typical 2.5MW wind turbine [39]

Therefore, the torque obtained on the rotor hub can be calculated by mechanical power extracted from the wind division by the main shaft speed.

5.2 Electromagnetic torque of generator

Since the wind turbine operates in the normal rated condition, the generator set up a static load torque in opposition to the wind turbine. In this report, the generator is DFIG, which is a typical asynchronous machine. The behavior of asynchronous generator is primarily determined by the steady-state torque/rotational speed characteristic of the fundamental-frequency field.

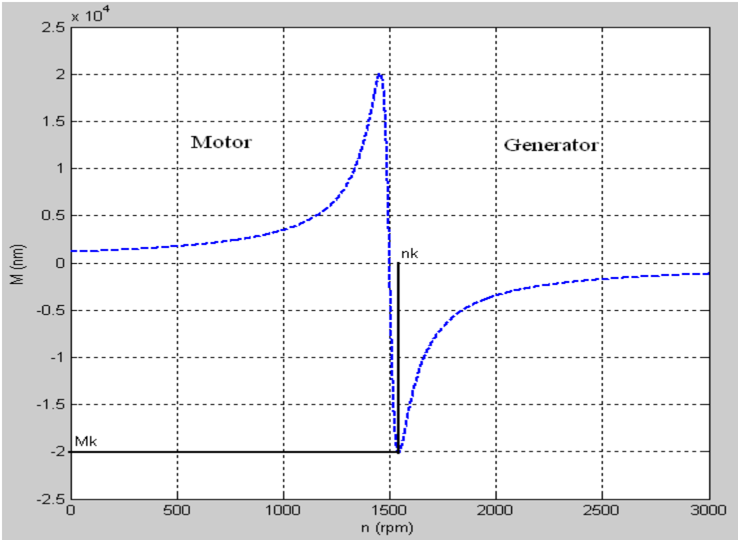

Figure 5.5 Torque/speed characteristic of an asynchronous machine

The air gap moment on the machine is generated over a characteristic line that is approximately determined according to $Klo\beta's$ equation for the asynchronous machine:

$$M \approx \frac{2*M_k}{\frac{s}{s_k}+\frac{s_k}{s}} \tag{5.10}$$

where M is the air gap moment on the machine, M_k the breakdown torque of asynchronous machine, s the slip and s_k the breakdown slip [40, 41].

$$s = \frac{n_1 - n}{n_1}$$

Where n_1 speed of rotating field or asynchronous speed and n the asynchronous machine rotor speed. In the generation operation mode, the generator rotor speed, n, exceeds the electrical grid speed n_1. Therefore the slip s is negative in generator mode. When the grid frequency is f, the electrical grid speed is given as: $n_1 = \frac{60f}{p}$, p the number of pairs of poles of the generator [40, 42].

From equation (5.10), one could see within the normal ranges, the machine characteristic heavily counts on the breakdown slip and the breakdown torque.

$$s_k = \frac{R_2'}{X_2'}\sqrt{\frac{R_1^2+X_1^2}{R_1^2+\sigma^2 X_1^2}} \tag{5.11}$$

And

$$M_k = \frac{3\mathrm{U}^2}{4\pi \mathrm{n}_0}\frac{1-\sigma}{\mathrm{R}_1(1-\sigma)+\sqrt{(R_1^2+\sigma^2 X_1^2)(1+\frac{R_1^2}{X_1^2})}} \tag{5.12}$$

Both equations can be determined by the relation of ohmic to leakage components, particularly in the rotor windings.

In equation (5.11) (5.12),

$$X_1 = X_h + X_{1\sigma}$$

$$X_2' = X_h + X_{2\sigma}'$$

$$\sigma = 1 - \frac{X_h^2}{X_1 X_2'}$$

where R_1 the resistance of stator winding (stator resistance), R_2' the rotor resistance of on phase of an asynchronous machine transformed on the stator side (rotor resistance), X_h the air gap reactance (magnetizing reactance), $X_{1\sigma}$ the leakage reactance of the stator winding, $X_{2\sigma}'$ the leakage reactance of the rotor winding in relation to the stator side, X_1 the stator leakage reactance, X_2' the rotor leakage reactance, σ the total leakage, n_0 the revolution of generator rotor (revolution per second), U the stator voltage (voltage) [40].

The Figure 5.6 depicts the method described above employed in AMESim. As seen in the picture, the port 1 is the angular velocity signal of high-speed shaft as an input for the generator model. While port 2 is the same as the aerodynamic toque system, the calculation torque from the generator.

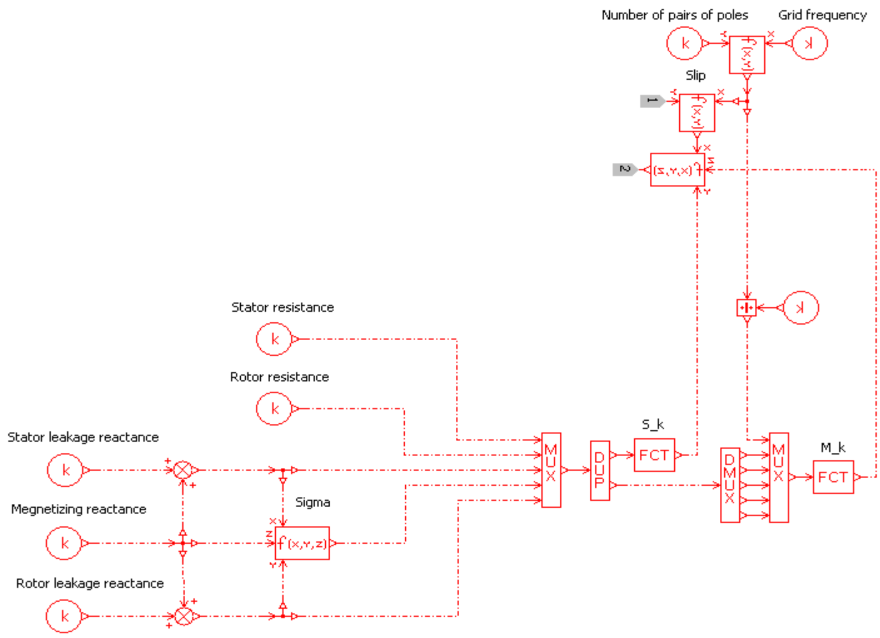

Figure5.6 The electromagnetic torque demonstration

In addition, there is another simple way to represent the generator response torque to the drivetrain. From the equation (6.14) later, it specifies the relationship between the torque of high speed shaft and that of low speed shaft. So generator obtains the value of toque which equals to the rotor hub toque times the total gear ratio while the direction is just opposite each other. Therefore, if there are no losses, all rotational components rotating constantly and the wind turbine running normally, the generator torque's absolute value is the product of the aerodynamic torque time the gear ratio and its sign is opposite to that of input torque.

6 Models of Dynamics of Drivetrain

6.1 Introduction to torsional vibration model

Torsional vibration is angular vibratory twisting of rotating components around its centerline that is superimposed on its rotary speed [30]. This type is not needed for many types of rotating machinery, particularly machines with a single uncoupled rotor. But for the wind turbine drivetrain, it is a quite long coupled rotating systems, which are the characteristics of the rotor hub, gearbox, brake, generator and that couplings instigate torsional rotary vibration problems.

6.2 Drivetrain model

The gearbox in the drivetrain is a mechanical system that transmits the mechanical power from the input driver to the output shaft, resulting in not only the change of the rotational speed but also the torque. Its characteristics apply in the wind turbine case, in which the gearbox lies between the rotor hub and the generator. Hence the gear ratio depends on the combination of the revolution of the main shaft and the generator requirement.

The low-speed shaft speed is a critical input for the pitch control subsystem, which is capable of rotating the blade around its own axis in order to regulate the mechanical power. In addition, the tip speed ratio is proportional to the low-speed rotational speed hence it is a significant factor of the mechanical power obtained from the wind energy. The tip speed is defined that the rotational speed of the tip of a blade divided by the actual speed of wind. The rotating speed increases always with the wind speed at the fixed pitch angle, but in the case of strong wind speed leading to the high mechanical torque in the gearbox, where it demands the pitch control to change the angle of attack in order to decrease the speed of the input shaft.

In most cases of wind turbine industry, the asynchronous machines are applied for the place of generator. The type of generator is widely used and operates in a broad speed range. The operational speed range of the induction generator is dictated by the connection grid frequency that the generator output links and the number of pairs of poles. In Europe, the most grid frequency is 50 HZ while it is 60 HZ in the United States. Nowadays, the pairs of poles for the induction generator used in wind turbine are typical from 2 to 3; therefore, the requirement input rotary speed of the generator rotor is between 1000 rpm and 1500 rpm for European area [40].

6.2.1 LMS Imagine.Lab AMESim

LMS Imagine.Lab AMESim was founded by the Imagine Company, which was obtained by LMS in 2007. Its platform is developed to build the one-dimensional (1-D) multi-domain system simulation. It offers various categories of pre-defined physical components which are ready to use. The validated libraries are possibly mechanical, electrical, hydraulic, or thermodynamic systems, etc from different areas.

The physical model is based on the individual components that are analytically validated, which does not need any information about the 3D geometry of the objective. The only thing that the user should do is a concept of model, only focus on describing the 1-D geometry representations. Therefore, the designer can spend most of treasure time on developing the creative and effective conceptual model. Before jumping into the complicated and time-consuming phase—detailed CAD geometry, the user could has the capability to simulate the overall performance of the multi physics model [43, 44].

The LMS Imagine.Lab AMESim is based on the Bond Graph Theory. In order to build the thorough and comprehensive system, the user has to go through the four mandatory steps. Firstly, in the sketch mode, the user is required to select the components needed for the model from the libraries. As soon as the model is complete, enter the second step-submodel mode, in which the physical submodels must be associated with each component. So the system is applied with a mathematical model. It is time to go for the third step-parameter mode; the parameters for the each component are ready to be set. Finally, the simulation mode can be activated and the whole simulation process is finished.

In the case of wind turbine, there are number components coming from the various physical areas, such as the aerodynamics, mechanical, electrical and electro-magnetic effects. The user could take the advantage of LMS Imagine.Lab AMESim for the sake of accurately studying the total behavior of the different subcomponents of wind turbine.

6.2.2 Functional components of drivetrain

In order to build the dynamic model for the drivetrain, one has to be clear that what the functional components (FCs) exist in the drivetrain within the concept and what the parameters for each functional component belonging to the drivetrain concept are. The constraints which connect the FCs of the drivetrain are also critical important for modeling. The typical concept of the drivetrain in the wind turbine is as follows:

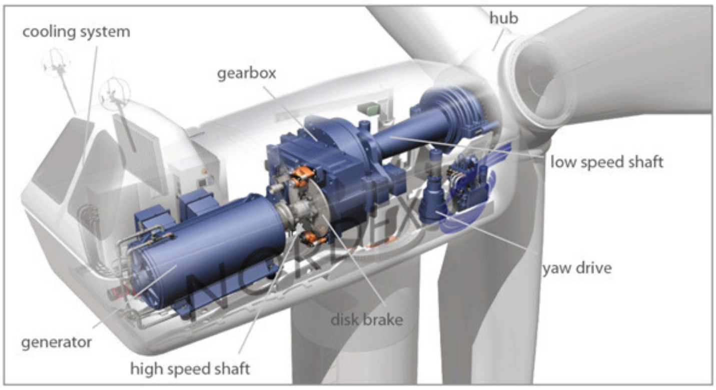

Figure 6.1 The schematic diagram of Vestas V112

This is the typical three point mounting suspension concept of the drivetrain from the Vestas V112, which is a representative for a modern wind turbine with a gearbox. Based on this configuration one is able to develop 1-D computational model in AMESim. The drivetrain has one main bearing integrated in the gearbox carrying the wind turbine rotor. The generator is a doubly fed induction generator (DFIG) and the gearbox design is a combination of two multi-stage planetary following one parallel spur gear. The wind turbine rotor is connected to the planet carrier of the first planetary stage. The stage has spur gears and the ring wheel is fixed in the gearbox housing. The housing is assumed to be rigid. The second gear stage in the gearbox is also a spur planetary stage. Its planet carrier is driven by the sun of the first stage and its ring wheel is also fixed in the gearbox housing. The sun of this stage drives the gear of the third gear stage, which is a parallel stage with spur gears. The pinion of this stage rotates at the speed of the operational range speed of the generator. A brake disk is mounted on this output shaft and a flexible coupling connects it with the input shaft of the generator. Since only the parallel gear stage causes a change in the direction of rotation, the high speed pinion and the generator rotate in the opposite direction of the rotor.

List the FCs in accordance with the order from the rotor hub to the generator rotor, which is a prerequisite before building the computational model for the drivetrain. The bearings are the crucial components in the drivetrain, especially for the analysis of the bearing misalignment and also the power losses at bearing positions. Hence one lists all the bearings in this drivetrain configuration.

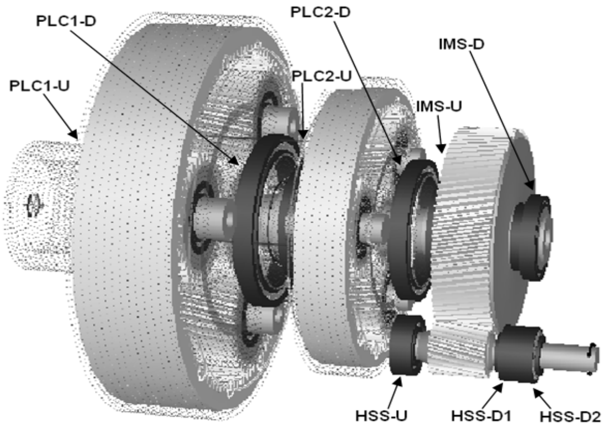

Figure 6.2 The two planetary gear stages with spur parallel gear

Table 6.1 List of bearings in the wind turbine gearbox

Label	Remarks
PLC1-U	First planet carrier bearing upwind
PLC1-D	First planet carrier bearing downwind
PLC2-U	Second planet carrier bearing upwind
PLC2-D	Second planet carrier bearing downwind
IMS-U	Intermediate shaft bearing upwind
IMS-D	Intermediate shaft bearing downwind
HSS-U	High speed shaft bearing upwind
HSS-D1	High speed shaft bearing downwind 1
HSS-D2	High speed shaft bearing downwind 2

First of all, the approach used to build the model in the AMESim is 1-D torsional vibration simulation multibody model. This approach mainly focuses on the overall performance of the drivetrain but not the loads in detail on internal components of the drivetrain. Based on this information, propose a method that combines the simply dynamic model and the detailed drivetrain model. A nonlinear dynamic case is simulated in the simplified low degree of freedom driveline model. Then the dynamic forces from the simplified dynamic model are employed in the detail drivetrain model, for instance, multibody six DOFs simulation dynamic model. This approach is called 'hybrid method' [5]. However, in this report, only the torsional vibration multibody simulation approach is studied.

In general, a static analysis cannot fully represent the loads during the transient events as it does not include the inertial force. In additional, there may be the dynamic loads due to the impulsive conditions, such as the gust from the rotor blade, the electrical or generator faults. That will definitely influence the loads condition of the drivetrain. The hybrid method is useful and efficient for predicting the internal component stress condition in the drivetrain during the dynamic external case. In the AMESim simulation environment, it is really convenient to build the 1-D multibody dynamic model for the drivetrain. The equations of motion for the dynamic model are solved numerically in the AMESim software. The aerodynamic torque at the rotor hub side and the electromagnetic torque at the generator side are considered as external loads, which can be modeled in AMESim

6.2.3 Angular and torque relationship of gear stages

The schematic of a typical power transmission system is represented in Figure 6.3. There are three parallel helical gear stages. The input torque M is transferred through the gear pairs to the output $\tilde{M}$.

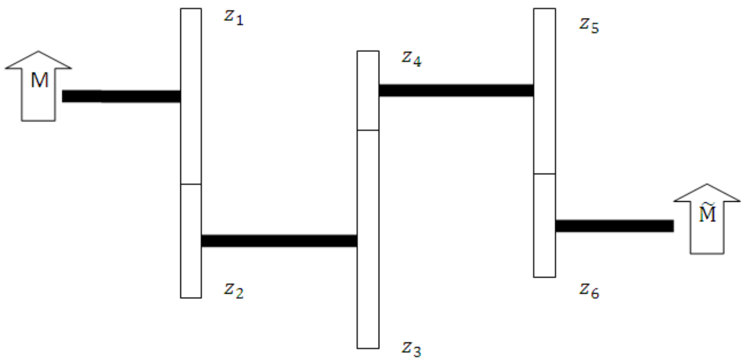

Figure 6.3 A typical speed increaser assembly

Following the power flow, the teeth numbers of gears are $z_1, z_2, z_3, z_4, z_5, z_6$. Based on the same principle, the rotating speeds of the each gear are named as $n_1, n_2, n_3, n_4, n_5, n_6$.

Before coming to calculate the torque relations, the hypothesis is set that the friction or heat loss is neglected, the rotary motion of inertia is ignored, and all the components are rigid bodies.

Focus on the first parallel gear pair, the input torque is $M_1 = M$, according to the conservation of energy,

$$P_1 * t = P_2 * t \Rightarrow P_1 = P_2 \Rightarrow M_1 * n_1 = -M_2 * n_2 \quad (6.1)$$

While for the gear pair, the speed at the meshing point for both gears is the same, so

Compatibility:

$$n_1 * r_1 = n_2 * r_2 \Rightarrow \frac{n_1}{n_2} = r_2/r_1 \quad (6.2)$$

The diameter of the gear is proportional to the number of gear teeth.

Here, we define the gear ratio $\frac{input\ speed}{output\ speed} = i$, applying the definition to the gear stages

$$n_2 = n_3, M_2 = M_3$$

$$n_4 = n_5, M_4 = M_5$$

First gear ratio,

$$i_1 = -\frac{n_1}{n_2} = -\frac{r_2}{r_1} = -\frac{z_2}{z_1} \quad (6.3)$$

Second gear ratio,

$$i_2 = -\frac{n_3}{n_4} = -\frac{r_4}{r_3} = -\frac{z_4}{z_3} \quad (6.4)$$

Third gear ratio,

$$i_3 = -\frac{n_5}{n_6} = -\frac{r_6}{r_5} = -\frac{z_6}{z_5} \quad (6.5)$$

Total gear ratio,

$$i = -\frac{n_1}{n_6} = -\frac{n_1}{n_2} * \frac{n_3}{n_4} * \frac{n_5}{n_6} = i_1 * i_2 * i_3 \quad (6.6)$$

From the equations (6.1) and (6.3), one can obtain,

$$M_2 = -M_1 * \frac{n_1}{n_2} = M_1 * i_1$$

Using the same way, one can get the following results,

$$M_3 = M_2, M_4 = M_3 * i_2 = M_2 * i_2 = M_1 * i_1 * i_2$$

$$M_5 = M_4, M_6 = M_5 * i_3 = M_4 * i_3 = M_1 * i_1 * i_2 * i_3$$

Therefore

$$\widetilde{M} = M_1 * i_1 * i_2 * i_3 = M_1 * i = M * i = -M * \frac{n_1}{n_2} * \frac{n_3}{n_4} * \frac{n_5}{n_6}$$
$$= -M * \frac{z_2}{z_1} * \frac{z_4}{z_3} * \frac{z_6}{z_5}$$

The schematic of a typical drivetrain employed in a wind turbine application is shown Figure 6.4. This is a multistage gearbox comprising of both two planetary sets and an external gear stage. The aerodynamic force coming from the turbine blade is the input to the transmission assembly through the carrier of the planetary set, which, in turn, drives the planet gears orbiting around the sun gear. The orbital movement of the planet gears makes the sun gear rotate at a higher rotary speed than that of the input carrier. The second planetary gear works in the same way as the first. The sun gear of the second is directly connected to a speed increaser pair, which consists of a pinion meshing with a smaller driven gear, rotating at a highest speed among all the gears. The input torque M is transferred through the gear pairs to the output $\widetilde{\mathrm{M}}$.

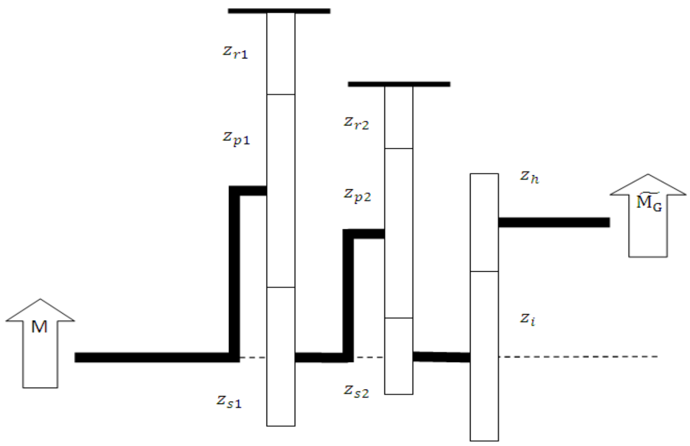

Figure 6.4 A typical drivetrain assembly applied in the wind turbine

Table 6.2 The parameters for the gear wheels

Name	Number of teeth	Rotating speed
Ring gear of first planetary gear	z_{r1}	n_{r1}
Planet carrier of first planetary gear	/	n_{c1}
Sun gear of first planetary gear	z_{s1}	n_{s1}
Ring gear of second planetary gear	z_{r2}	n_{r2}
Planet carrier of second planetary gear	/	n_{c2}
Sun gear of second planetary gear	z_{s2}	n_{s2}
Intermediate gear	z_i	n_i
High speed gear	z_h	n_h

Before coming to calculate the torque relations, the hypothesis is set that the friction or heat loss is neglected, the rotary motion of inertia is ignored, and all the components are rigid bodies.

Focus on the first planetary gear stage, the input torque is $M_1 = M$, according to the conservation of energy,

$$P = P_{r1} + P_{s1} \tag{6.7}$$

While the ring gear is fixed to the gearbox housing,

So

$$n_{r1} = 0 \tag{6.8}$$

From the equations (6.7) (6.8)

$$P = P_{s1} \Rightarrow M * n_{c1} = M_{s1} * n_{s1} \tag{6.9}$$

The diameter of the gear is proportional to the number of gear teeth.

Here, we define the gear ratio $\frac{input\ speed}{output\ speed} = i$, applying the definition to the gear stages

$$n_{s1} = n_{c2}, M_{s1} = M_{c2}$$

$$n_{s2} = n_i, M_{s2} = M_i$$

First gear ratio,

$$i_1 = \frac{n_{c1}}{n_{s1}} = \frac{1}{1+z_{r1}/z_{s1}} \tag{6.10}$$

Second gear ratio,

$$i_2 = \frac{n_{c2}}{n_{s2}} = \frac{1}{1+z_{r2}/z_{s2}} \tag{6.11}$$

Third gear ratio,

$$i_3 = -\frac{n_i}{n_h} = -z_h/z_i \tag{6.12}$$

Total gear ratio,

$$i = \frac{n_{c1}}{n_h} = -\frac{n_{c1}}{n_{s1}} * \frac{n_{c2}}{n_{s2}} * \frac{n_i}{n_h} = i_1 * i_2 * i_3 \tag{6.13}$$

From the equations (6.9) and (6.10), one can obtain,

$$M_{s1} = M * \frac{n_{c1}}{n_{s1}} = M * i_1$$

Using the same way, one can get the following results,

$$M_{c2} = M_{s1}, M_{s2} = M_{c2} * i_2 = M_{s1} * i_2 = M * i_1 * i_2$$

$$M_i = M_{s2}, M_h = M_i * i_3 = M_{s2} * i_3 = M * i_1 * i_2 * i_3$$

Therefore

$$\widetilde{M}_g = M * i_1 * i_2 * i_3 = M * i = -M * \frac{n_{c1}}{n_{s1}} * \frac{n_{c2}}{n_{s2}} * \frac{n_i}{n_h}$$

$$= -M * \frac{1}{1+z_{r1}/z_{s1}} * \frac{1}{1+z_{r2}/z_{s2}} * \frac{z_h}{z_i} \Rightarrow \widetilde{M}_g = -\frac{M * z_h}{\left(1+\frac{z_{r1}}{z_{s1}}\right) * \left(1+\frac{z_{r2}}{z_{s2}}\right) * z_i} \tag{6.14}$$

6.3 Different levels of progressive modeling

6.3.1 Overall wind turbine description

As discussed in Chapter 2, the typical gear-driven, modular concept employed in the wind turbine industry is introduced to develop the 1-D dynamic torsional model. The concept chosen in this report is a classical representative of the modern wind turbine industry standard. The drivetrain configuration is the same as the structural model in Figure 6.5, which is the three-point supporting drivetrain. The planet carrier end bearing for the main shaft is integrated in the gearbox housing. This concept consists of the rotor hub, a low-speed shaft, gearbox, a high-speed shaft, brake, coupling and generator.

The generator is a type of DFIG as mentioned in previous paragraph 6.2.2. The gearbox design follows the typical configuration of two multi-stages planetary and one parallel stage with spur gears. The location of the mechanical brake is in conjunction with the gearbox on the high speed shaft, which isolates the gearbox with regard to the generator and the electrical grid during the period of regular maintenance and high winds.

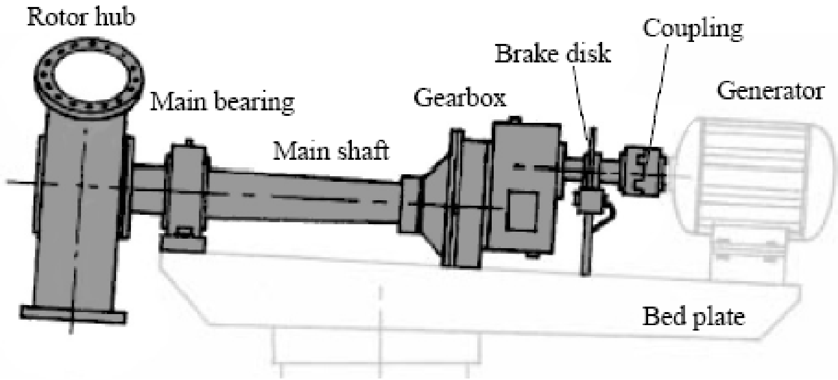

Figure 6.5 Layout of a wind turbine drivetrain [45]

The wind turbine is an upwind horizontal axis, three-blade concept with rated power at 2 MW, which is the popular overall configuration currently. The blade diameter of this wind turbine is 80 m. The size of the turbine is closed to the offshore wind turbine that is the new direction of the development of wind turbine technology. Offshore wind turbine demands the requirements not needed for onshore turbine due to the harsh climatic environment exposed in the sea. Therefore, it is a profound meaning for the development of the offshore wind turbine that employing the large size of wind turbine in the report.

6.3.2 Stage 1-Drivetrain model with simplified multi-stage gearbox

At the first design stage, all the components of the wind turbine are modeled in a relative simple way. The model comprises three main sections, the first one stands for the aerodynamic toque obtained from the rotor hub, the second one stands for the three-stage gearbox, the third one stands for the electromagnetic torque coming from the generator rotor. Each gearbox parts are included in the model built in the AMESim, such as the shafts, gear wheels. The wind turbine only has one DOF per each component modeled in the simulation. The coupling is implemented as a rigid connection between two adjacent bodies. The model focuses on the torsional vibration hence the torque around the axis is the only force transferred via the drivetrain.

Though this is the simplest 1-D dynamic model, it is of extreme importance for the validation of the way that is employed to build the model and reference comparison of the subsequent stage models. What is more, this model could be used to create the load condition of the drivetrain by means of aeroelastic codes, which is better and more accurate than that results from the two-mass simply dynamic model. In that model, one mass moment of inertia represents the rotor, the other represents the generator, which are connected each other with one torsional spring damping connector. The gearbox influence is included in the equivalent stiffness of shaft and inertia of generator that are both proportional to the square of gear ratio [29].

The schematic of the model is shown in Figure 6.5. The flexible coupling can be considered as only flexible in torsional direction, hence, which is represented as a torsional spring damping joint. While the field data of coupling is difficult to obtain the coupling is regard as the rigid body. The mechanical brake mounted on the high speed shaft is modeled as an additional mass of inertia part.

The model in this stage takes into account the torsional deflection of the shaft and the contacting deflection of the gear teeth along the action line of contacting force. However, the other torsional compliances, such as bending of the blades, bending of the shaft due to the gravity, backlash of the gear wheels, flexibility of the bearing etc, are not considered in the system.

6.3.2.1 Shaft stiffness

With regarding to the shaft, in the AMESim, there are only two types of shafts: one is a very simple shaft and the other is an elastic rotary shaft. The former is that the torque or rotary velocity is passed through the shaft without any change. While the latter considers the stiffness and damping, so this sort is picked to represent the torsional stiffness of all the shafts in the wind turbine.

The shafts are modeled as a lumped point. The influence of shaft length and diameter variation along the axis is ignored in this model. Therefore the shaft is divided into two equal sections, standing for the two separate sub-shafts that are connected by the lumped effective torsional stiffness and damping element. In this way, it represents the overall behavior of the shaft, whereas neglecting the internal performance of the shaft.

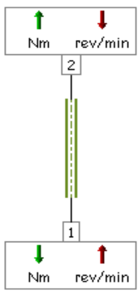

Figure 6.6 TRSH1A-Shaft with rotary spring and damper

In the parameter mode when building the model in AMESim, the input parameters of the TRSH1A submodel are the relative angular displacement, the spring's torsional stiffness and damping. The spring stiffness of the shaft must be positive and the damping coefficient can be zero or positive. During this design stage, the damping coefficient is set to be zero. When the simulation is done, the relative angular displacement, torques and rotary velocity at both ports can be seen in the variable list of the TRSH1A shaft [46].

As a matter of fact, the shaft with stiffness and damping has the same function as rotary spring and damper (with state variable) –RSD00. The Figure 6.7 demonstrates what RSD00 looks like and it acts exactly the same as TRSH1A.

RSD00A is also a rotary spring damper. But there is a difference that the user should pay attention to; it computes the relative angular displacement directly from the angles passed at ports whereas RSD00 computes it from the rotary velocities. However, RSD00A is recommended to be used in low to intermediate rotary speed model. Therefore, if applying the rotary spring and damper in the wind turbine, RSD00 is a better choice.

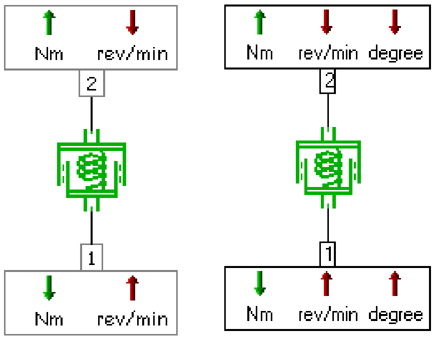

Figure 6.7 RSD00-rotary spring and damper (with state variable) & RSD00A-rotary spring and damper (no state)

6.3.2.2 Gear meshing stiffness

The contact force between the gear wheels can be calculated by means of considering or not nonlinear contact stiffness, variable number of contacting teeth, backlash. Selecting the assumption has a large impact on the performance of the gear meshing and more important is the behavior of dynamics of gears.

At this design stage, the constant gear meshing is assumed. The contact between the gear wheels is modeled as a spring damper. The mode shape for the gear meshing frequency is therefore possible to be simulated. The stiffness value is the gear contact stiffness not the intrinsic stiffness of meshing gears; if the stiffness referring to two gears is denoted as K_1 and K_2, the effective stiffness is calculated as follows:

$$K_{gm} = \frac{K_1 K_2}{K_1 + K_2}$$

The contact viscous coefficient is fixed at the critical damping, which could be expressed by the following equation:

$$C_{gm} = 2\xi_{gm}\sqrt{K_m J}$$

Where ξ_{gm} the damping ratio, K_m the middle contact stiffness and J the mass moment of inertia of the gear [43].

Constant gear meshing assumes the stiffness of the tooth is constant along the tooth. This approach does not take into account the variable number of gear contacts, hence the stiffness is linear. In addition, the backlash is ignored in this stage for the simplification of model. Therefore, this model is at the most conservative state; due to the only contact assumption is constant stiffness.

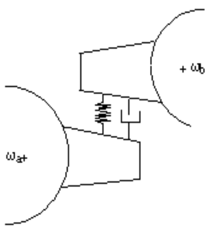

Figure 6.8 The sketch of constant gear meshing stiffness

With respect to the planetary, AMESim library supplies various types of planetary for the users. The category of complete planetary geartrain-simple is a simple submodel of planetary with no gear meshing stiffness, inertia and etc. Another type called complete planetary geartrain-efficiency supplied by user is almost the same as the first one. The gear meshing efficiency differentiates the former type. The last one is chosen for the wind turbine model, that is, complete planetary geartrain-gear backlash with simple contact. AMESim makes it convenient to model the gear meshing stiffness. In the parameter mode, double-click the planetary icon, the Change Parameters dialog box is created as Figure 6.9. For this model, due to ignoring the backlash, the total clearance between sun and planet gears, ring and planet gears is set to be zero. The contact stiffness and damping are also readily to be changed.

The parallel gear stages employ the three ports gear submodels. They also have three types, the same as the planetary submodel. TRGT00C–3 port gear (velocity input port 1) is picked to represent the parallel gear. In the parameter mode, open the Change Parameters dialog box of this submodel shown in Figure 6.10, besides set the backlash, gear contact stiffness and losses, the type of gear can be determined by changing the value of helix angle. If the helix angle is zero, the gear type is spur gear; otherwise, the gear could be the helical gear. However, in the planetary Change Parameters dialog box, the teeth angle is fixed already by factory default.

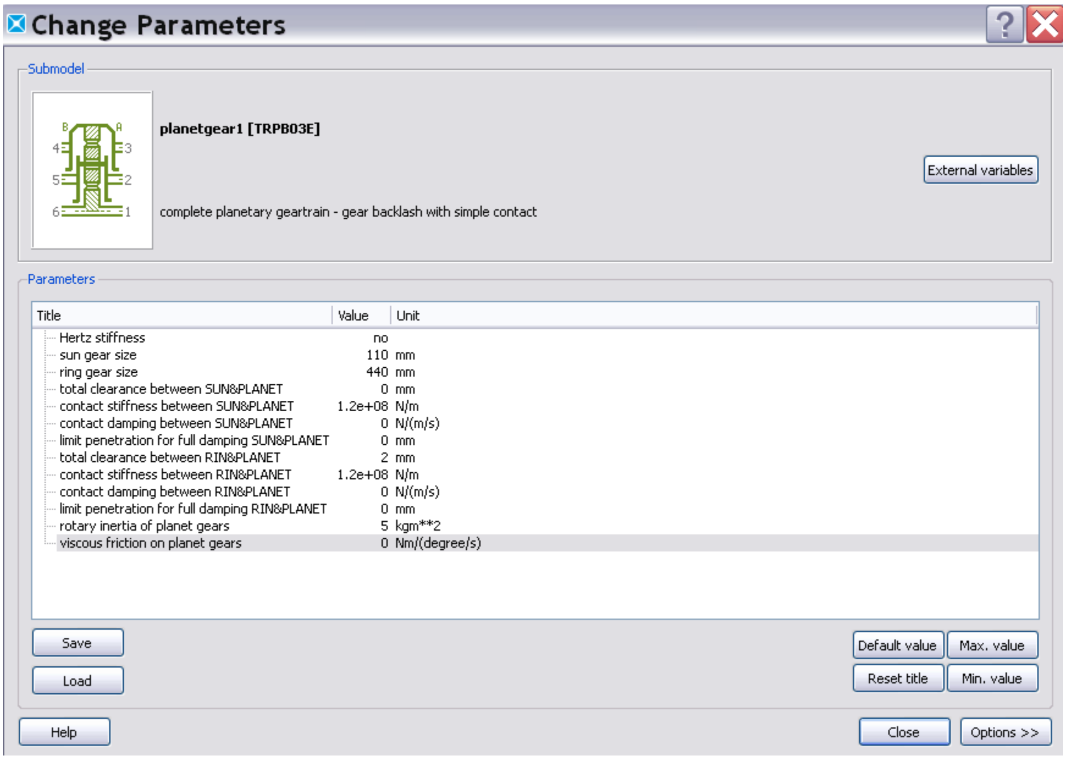

Figure 6.9 The Change Parameters dialog box of planetary

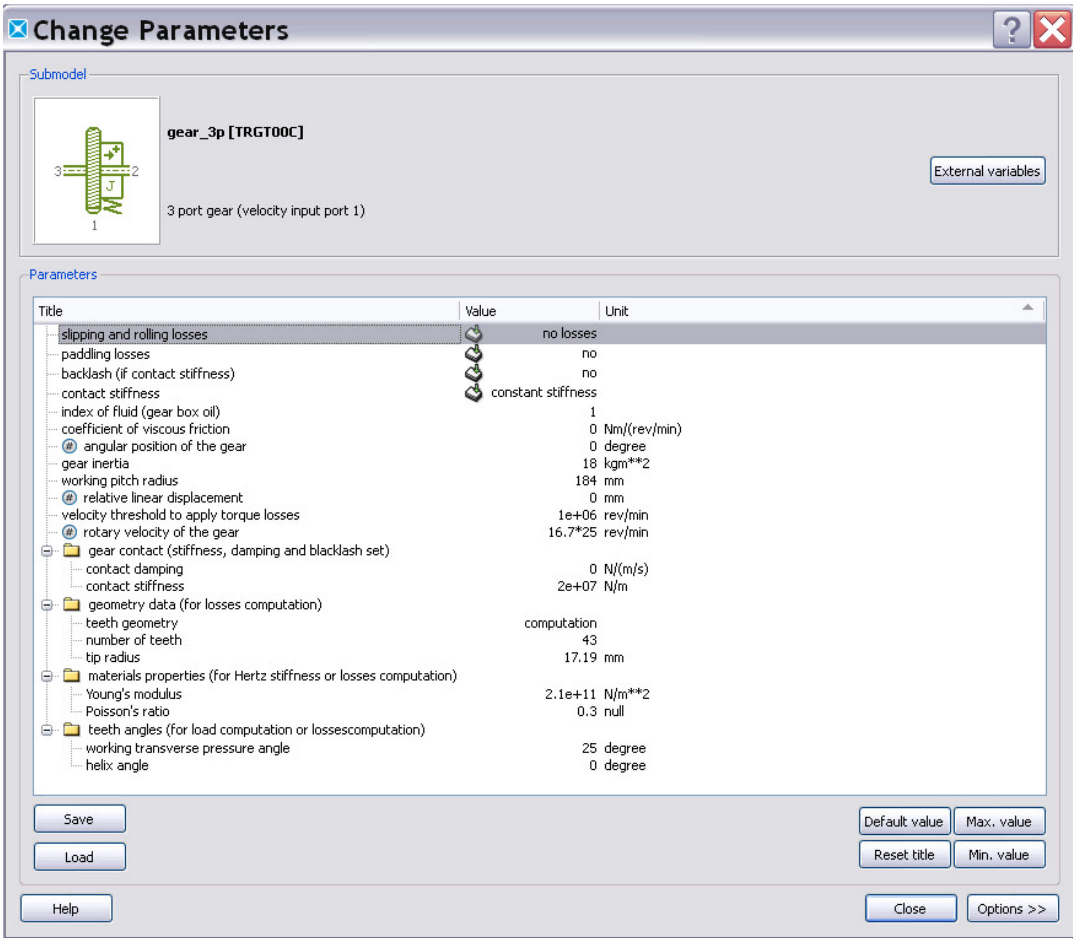

Figure 6.10   The Change Parameters dialog box of 3 port gear

6.3.2.3 Inertia

The inertia of wind turbine components are considered as lumped and the data is coming from the experimental test and paper references.

The rotor hub and generator are lumped at each of the gearbox's two end points. Both concentrated mass moment of inertia are optionally added at the low and high speed shaft ends as approximate assumption for blade and generator rotor subcomponent.

As mentioned in 6.3.2.1, the shaft is subdivided into two equal parts connected by a rotary spring damper [30]. The connection means between the shaft and gear, generator rotor and rotor hub are characterized as ideal. However, the relative large clearance effect of the spline between shaft and gear, which leads to the nonlinear stress and shaft torsional stiffness, is set to be neglected [47]. In this model, half the shaft polar moment of inertia is mounted on the end points of shaft. The two independent sections of the shaft are joined by a spring damper; therefore the overall behavior and interaction between the two sections of shaft are simulated by AMESim.

In AMESim, the rotary load could be classified in three categories: rotary load without friction, rotary load with angle as output and rotary load with friction. In the first stage, the friction loss is not included. These two types of RL02–rotary load with two shafts without friction and RL02A–rotary load with two shafts without friction (angle as output) are taken into account [46]. As shown in Figure 6.11, the distinction between RL02 and RL02A is the same as the shaft referred to in 6.3.2.1. An angular displacement is passed at RL02A ports; consequently, RL01A is not suitable for the high rotary velocity system, otherwise the angles at port may arrive at enormous high values quickly resulting in the numerical issues.

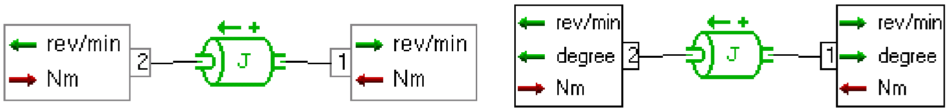

Figure 6.11 RL02-rotary load with two shafts without friction & RL02A−rotary load with two shafts without friction (angle as output)

As shown in Figure 6.12, the lumped inertia of the shaft is interpreted in the graphic way. Two-equal polar moments of inertia are connected by an elastic rotary shaft, that is, a rotary spring damper. If incorporate the shaft model in the whole system of wind turbine, the inertia of shaft can be optionally added at the stations where other rotating parts, such as gears, mechanical brake, blade rotor and generator rotor are probably modeled in AMESim.

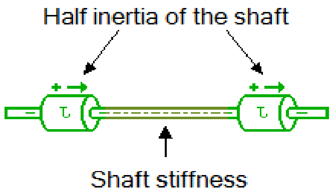

Figure 6.12 Representation of the shaft

With regard to the inertia for the gearbox, as shown in Figure 6.10, there is no inertia for the gears apart from the rotary inertia of planet gears in the planetary gear. For the purpose of making up this issue, an additional rotary load with two shafts is added to the ports for the planetary gear. In this way, the inertia of the planet carrier and sun gear is taken into consideration. The approach is also implemented for the parallel gear stages if the Change Parameter dialog box of gear wheel does not contain the gear inertia.

Figure 6.13 is a graphic representation of the planetary stage with inertia implemented. Due to the inertia of planets already exists in the planetary gear chosen for the model in stage one, the way demonstrates the planetary thoroughly. The two inertia submodels are the implementation for the TRPB03E-complete planetary geartrain-gear backlash with simple contact. The ring gear is fixed to the gearbox housing that is assumed a rigid body in this model, in the model, a zero torque source and a zero angular speed source are connected to the ports of the ring gear to represent the behavior of the ring gear. On the other side of the planet carrier and the sun gear, a zero torque source is joined to complete the planetary gear train.

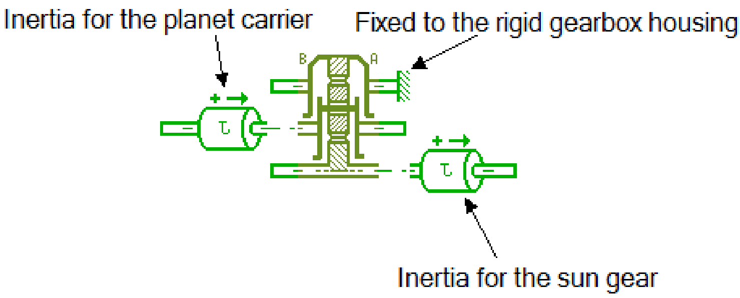

Figure 6.13 The sketch of planetary with supplementary inertia

Figure 6.14 is the last part of the gearbox. At the top level left, the inertia of gear is represented by a rotary load. In the same means, at the port of pinion another rotary load is attached. However, if the 3 port gear submodel does comprise the gear inertia, the rotary load is left out.

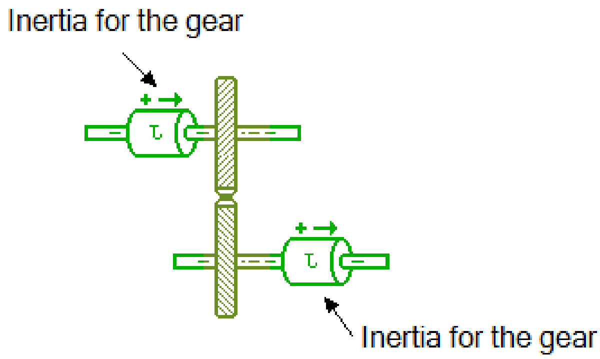

Figure 6.14 The sketch of 3 port gear with supplementary inertia

From the above discussion, all internal components of gearbox are taken into account for this model. This demands the physical parameter for the components influencing the dynamic performance of the drivetrain.

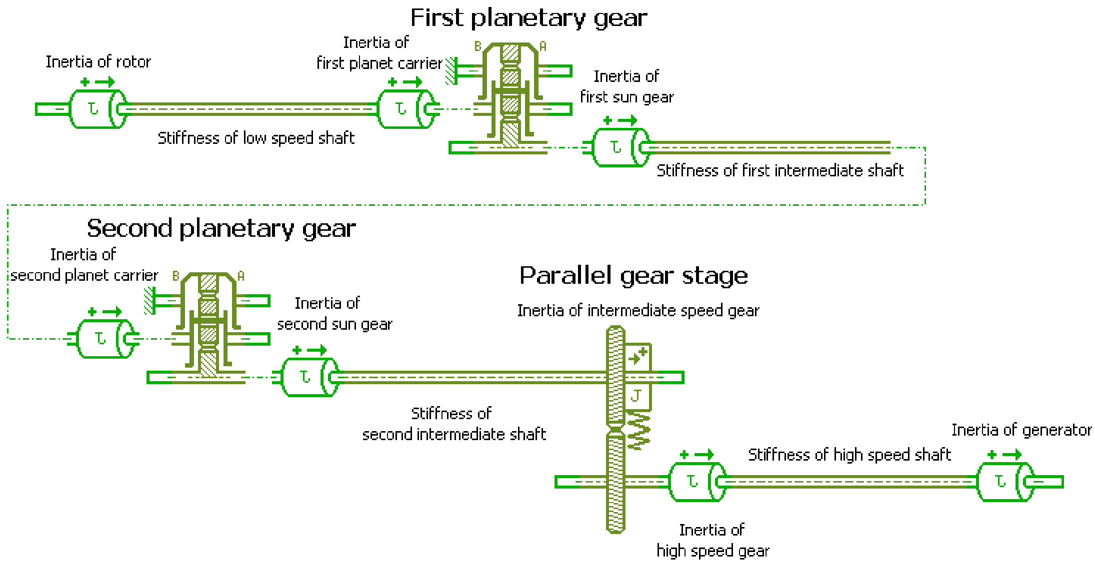

Figure 6.15 The drivetrain topology for Stage 1

Figure 6.15 is a comprehensive configuration of the drivetrain, which is 1-D multibody dynamic model. The front-end of the system is inertia that represents the rotor hub and at rear-end of model there is generator rotor inertia. In the diagram, the aerodynamic torque and electromagnetic torque are constituted by two zero torque force sources in order to facilitate the description of the drivetrain. Between these two inertia, the gearbox account for the transmission of the mechanical power from the aerodynamic force. The planet carrier of the first planetary receives the input torque from the low speed shaft and the ring gear is fixed to the gearbox housing. The second planetary planet carrier is driven by the sun gear of first planetary. The ring gear of this stage is also connected to the rigid housing. This sun gear rotates the gear of the parallel gear stage, and finally the pinion is spinning at the angular speed of the generator. In the model, due to the gear submodel of parallel gear stage include the inertia parameter, the rotary load is ignored for the gear but for the pinion gear it still requires the rotary load. The half inertia of the each shaft is lumped at both end points of the shaft, which is added to the stations of the drivetrain. The representation of the mechanical brake is an additional inertia at the high speed shaft.

6.3.3 Stage 2-Multi-stage gearbox with backlash and Hertz stiffness

At this stage, most of submodels are the same as the Stage 1, except for the gear contacting characteristics. The parameters of the gearbox are entered at the parameter mode, which could result in the contact element of taking into account the Hertz stiffness, backlash and rotating direction of the gear wheels. The shaft is an elastic rotary shaft (as the previous stage) with the lumped inertia.

The ring gear is still fixed to the gearbox housing with rigid connection. Because of the backlash of the gears, the direction and magnitude of the force on the tooth changes with time and each revolution, that is of extreme importance to the dynamic behavior of the gear meshing and also the gear noise generated by gear impact.

6.3.3.1 Shaft stiffness

As the model in the Stage 1, the shafts are assumed to be average diameter steel circular beams, which are modeled by a rotary spring damper with two equal inertia lumped at the end points. The influence of the steps and stress variation is ignored. Other detail information, see the Section 6.3.2.1.

6.3.3.2 Gear meshing stiffness

In this model, the gear meshing stiffness is modeled in a more realistic approach which is done by the AMESim simulation code. The stiffness result is calculated by the gear primitive parameters. In addition, some structural properties are also provided to describe the characteristic of gear meshing accurately. The submodels of TRPB03F–complete planetary geartrain and TRGT00C–3 port gear take into consideration of no linearity and variation in stiffness resulting from the increase of contact area with the increase of teeth deformation.

Hertz stiffness is put in series to the contact stiffness:

$$\mathrm{K(x)} = \frac{\mathrm{K_{hertz}(x) \cdot K}}{\mathrm{K_{hertz}(x) + K}}$$

Where $\mathrm{K_{hertz}(x)} = \frac{2}{3}\sqrt{E_q \cdot R \cdot X}$, where E_q is the equivalent Young modulus. It is also called modulus of elasticity calculated by the Young modulus, Poisson ratio of gear 1 and 2.

$$\mathrm{E_{eq}} = \frac{2}{\frac{1-\upsilon_1^2}{\mathrm{E_1}} + \frac{1-\upsilon_2^2}{\mathrm{E_2}}}$$

The teeth backlash is included in the system. AMESim utilize two elastic endstops at the right and at the left of the teeth. There is an interval time when the contact compression is negative. At this period, the contact force is zero. When the contact compression is little, the force is proportional to the torsional stiffness. In other cases, the spring damping force is calculated. Therefore the contact force can be expressed in following way:

$$F_b(x) = \begin{cases} 0 & \text{if } x \leq 0 \\ K \cdot x & \text{if } 0 < x \leq tol\ (tolerance) \\ K \cdot x + C \cdot \dot{x} & \text{else} \end{cases}$$

Where K is the current contact stiffness, C is the contact damping and tol is the limit penetration to apply the full damping [43]. All these parameter could be set in the Change Parameter dialog box at the parameter mode of system.

In this stage, the damping of the gear stages is considered in order to fully analyze the influence of backlash to the dynamics of gears and the local force between the gear wheels.

6.3.3.3 Inertia

The inertia of components is obtained by the assumption based on the field data and reference paper. The approach that models for the inertia is the same as that in the Stage 1. There is no difference between the inertia modeling manner of Stage 1 and this stage.

The topology is the same as Stage 1, as shown in Figure 6.16. However, at the parameter mode, there is a step distinguishing the model from that at Stage 1.

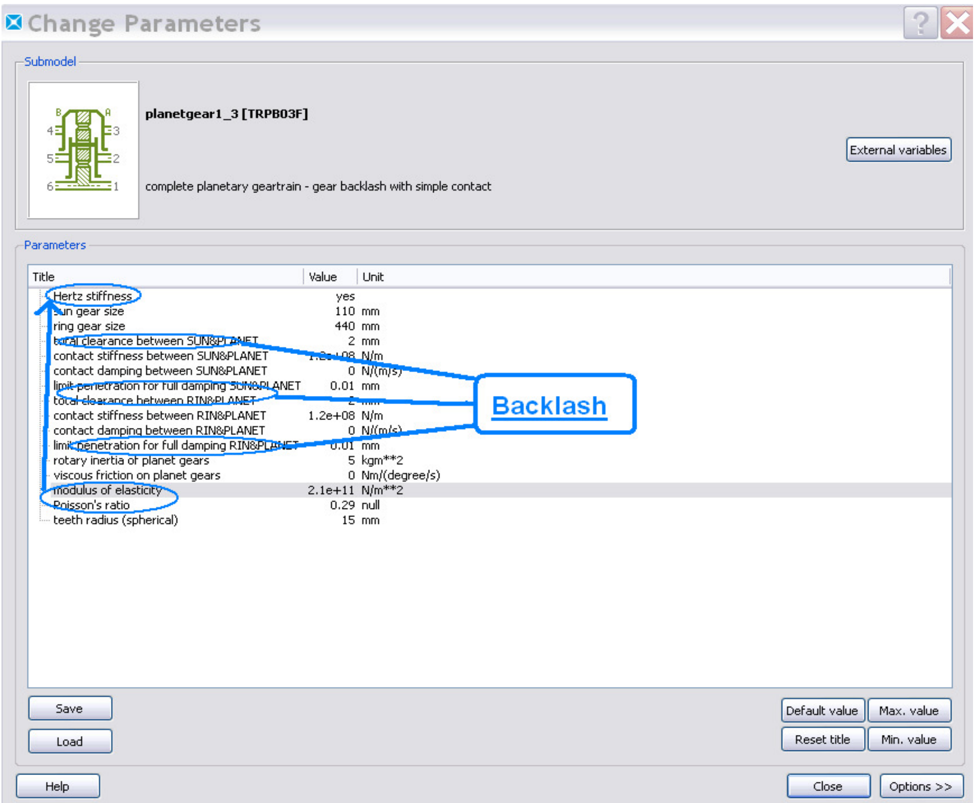

Figure 6.16 The sketch of Change Parameter dialog box of TRPB03F

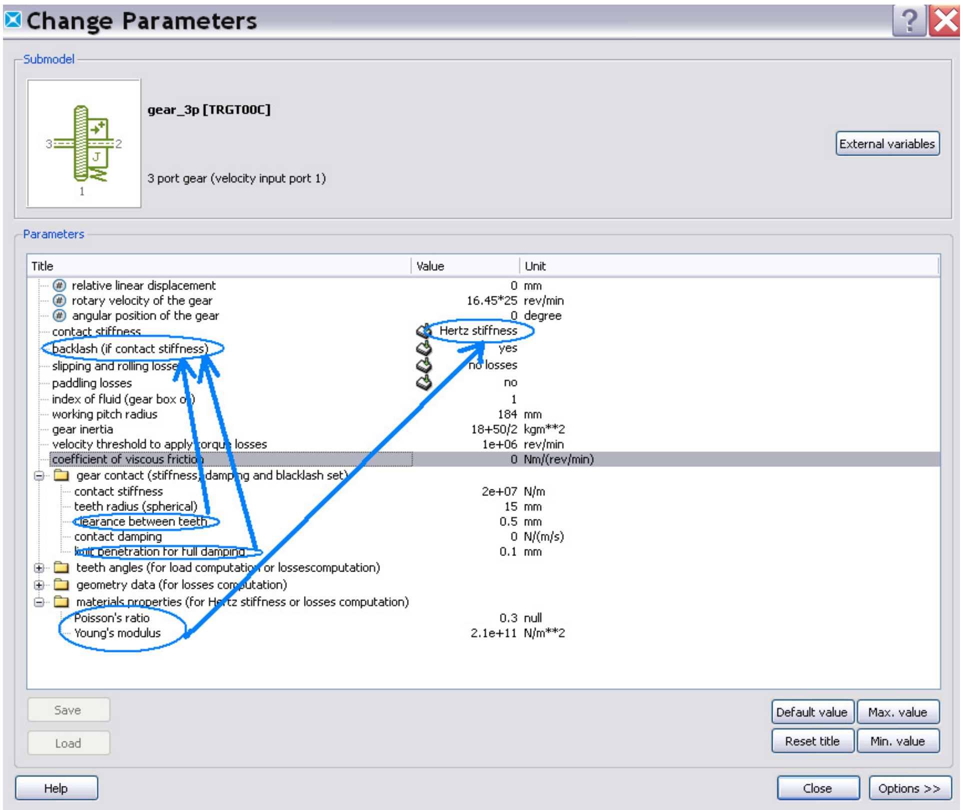

Figure 6.17 The sketch of Change Parameter dialog box of TRGT00C

Double click on the submodels of TRPB03F–complete planetary geartrain and TRGT00C–3 port gear take, the user can choose the type of contact stiffness and backlash, then supply the material property in order to make the simulation of Hertz stiffness and backlash done successfully.

If choosing the backlash on, the clearance between teeth and limit penetration for full damping will automatically pop up to facilitate to set values for calculation of contact force taking into account backlash as discussed in 6.3.3.2. In the same way, setting the Poisson’s ratio and Young’s modulus is to obtain the Hertz stiffness, which is more closed to the reality than the constant stiffness. Therefore, this model of Stage 2 is supposed to supply more information than that of Stage 1, especially referring to the load force inside the gearbox.

6.3.4 Stage 3-Drivetrain with bearing losses

The final stage adds the power losses to the system built in Stage 2. In general, the power loss can be coming from both the bearing and gear stages locations. In AMESim, the following physical phenomena contribute to the losses: gear losses and bearing losses. The former consists of gear paddling losses, gear slipping losses, gear rolling losses, gear contact losses. The gear paddling losses are highly depending on the oil property, the oil immersed gear height, the teeth geometry and the rotary velocity. The other three gear losses are determined by the oil property, the teeth geometry, the teeth load and the rotary velocity of gears. However, TRPB03F that is the most complicated physical submodel for the planetary does not contain the parameters for the gear losses in the Change Parameter dialog box. Therefore, for the sake of comparison, in the Stage 3, the power losses are only derived from the bearing losses.

The approach utilized here to calculate the power losses is to compare the absolute value of the products of the torque and the angular speed at the locations where are input and output shafts of the gearbox. The difference between these two numbers is equal to the power loss due to bearing in this model.

6.3.4.1 Parameters

As the model in the previous stages, the shafts are assumed to be average diameter steel circular beams, which are modeled by a rotary spring damper with two equal inertia lumped at the end points. Detail information, see the Section 6.3.2.1.

In this model, the gear meshing stiffness is the same as the approach in Stage 2. The Hertz stiffness is calculated by the gear primitive parameters, done by AMESim codes. The main material parameters for the Hertz stiffness are Young's modulus and Poisson ratio of contact gears.

In addition, the teeth backlash is taken into account in the same way as Stage 2. In parameter mode, the user could change the values of clearance between gears and the limit penetration to apply the full damping for introduce of backlash in the system. There is more information in Section 6.3.3.2.

All components inertia is obtained by the assumption based on the field data and reference paper. The manner to build the model for inertia is discussed in Section 6.3.2.3.

6.3.4.2 Bearing loss calculation

The losses parameters of the bearings are utilizing supplier documentation. For spherical roller bearing the TIMKEN catalogue gives [43].

Table 6.3 TIMKEN catalogue data

Name	Value
Frictional factor dependent on speed, f0	7
Frictional factor dependent on main load, f1	0.00049
Frictional factor dependent on secondary load, f2	0
Characteristic ratio between axial and radial loads, e	$10/(8 * cot(\alpha))$
Axial load factor (when Fa/Fr<=e), Y	0
Radial load factor (when Fa/Fr<=e), X	1
Axial load factor (when Fa/Fr>e), Y	$0.8 * cot(\alpha)$
Radial load factor (when Fa/Fr>e), X	0

Assuming default oil properties, working transverse pressure angle of 25 degrees, the bearing power losses can be calculated by AMESim automatically.

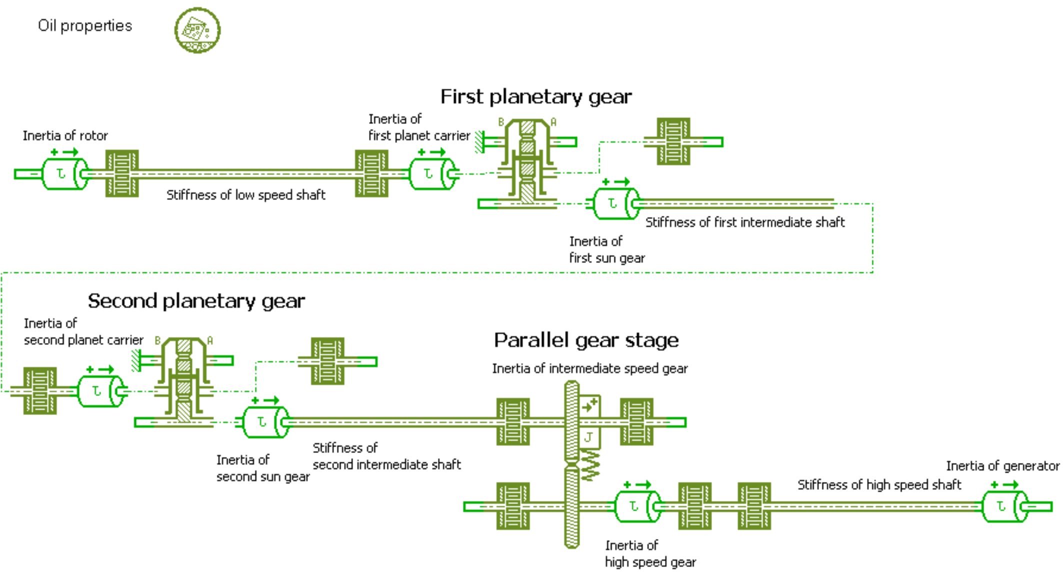

Figure 6.18 The drivetrain topology for Stage 3

Figure 6.18 is a demonstration of the model for Stage 3. As the previous stages, the aerodynamic torque and electromagnetic torque are constituted by two zero torque force. The configuration of the bearing is discussed in 6.2.2, which is interpreted comprehensively in the Figure 6.2. The type of the bearing is the spherical roller bearing. It is stilled used massively in the wind turbine industry, though; the Siemens Wind Power has discovered one breakthrough that the standard use of spherical roller bearings seems to have been a mistake [48].

7 Analysis of Drivetrain in Wind Turbine

The chapter presents the simulation results of the computational models of drivetrain in AMESim. There are different aspects to analysis the dynamic models of various complexities as described in Chapter 6.3. The model at Stage 1 is one simplest torsional system of drivetrain with the only flexibilities existing in the rotating shafts and the gear meshing. Stage 2 takes the advantage of AMESim consisting of the damping coefficient of shafts and gear contact, backlash of the gear stages and also more realistic gear contact stiffness-Hertz stiffness. At the last stage, the model is based on the previous model, further introducing the bearing loss.

In this part, the simulation is divided into three ways to demonstrate the dynamic characteristics of the gearbox. The first section deals with gearbox model without the extension in order to do free torsional vibration analysis. It is interesting to examine the varying behaviors of the model without backlash and that with backlash and Hertz stiffness, involved the models of Stage 1 and Stage 2. The torsional multibody methodology facilities the determination of both eigenvalues and mode shapes, so these are required to be presented to check the differences due to the complexity of the models. Then the second section extends the model with extra components at the rotor and generator sides for transient vibration dynamics. The load condition of gearbox could be highly rigorous quite different from drivetrain applications of other industries. The operation load duration is a time history of transferred torque in the gearbox, including both normal condition and fault condition. The latter one results in the transient load case. The transient conditions may come from the short circuits in the electrical network, gusts resulting in severe load case and reverse torque due to emergency stop etc. Then choose one type of transient load case applied in the dynamic model in order to yield the insight in the drivetrain behavior and much detailed information. The extension of Stage 1 and Stage 2 models are demanded to describe the external forces during a transient load case accurately including the aerodynamics and generator. Finally, the steady state vibration analysis is focusing on the comparisons of power losses using different drivetrain models. The models in line with Stage 1 and Stage 3 are utilized to compare the influence of the bearing loss.

7.1 Free torsional vibration

The models of Stage 1 and 2 are used to compare the free torsional vibration results in this section. In this part, the Linear analysis mode is selected for the eigenvalue and mode shape.

The following Figure 7.1 is the sketch of the gearbox model for the free vibration analysis. The model is taking into account the inertia of the rotor and generator and there is no torque input to the system. The initial state of the rotary load and the gear stages is set at a reasonable state.

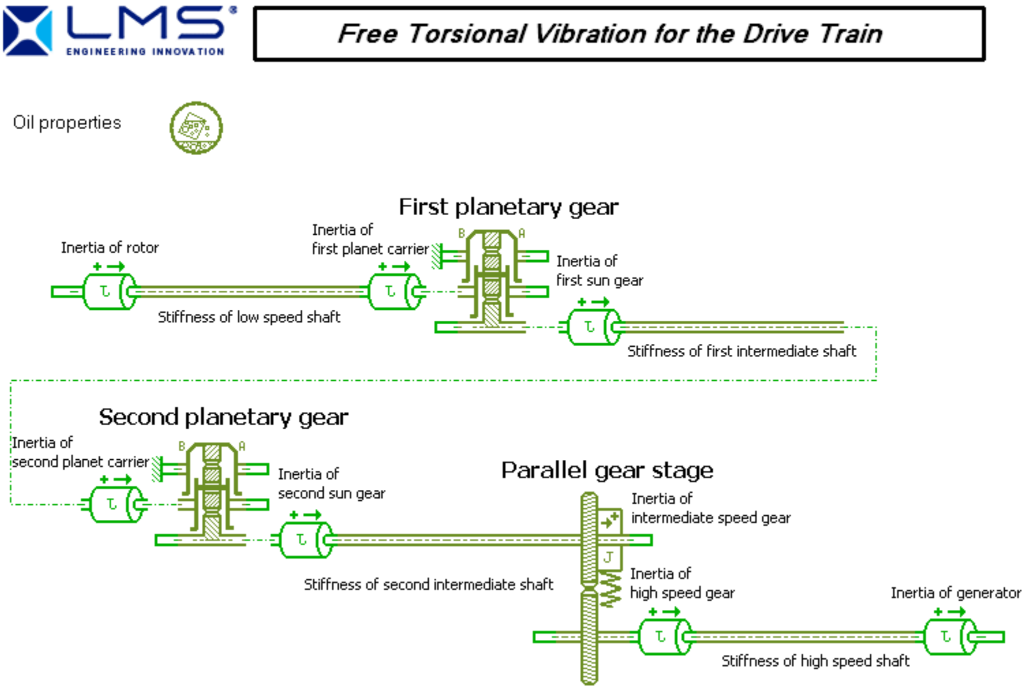

Figure 7.1 The sketch of the gearbox model

Table 7.1 Initial state

Name	Value (rev/min)
Rotor	16.45
First planet carrier	16.45
First sun gear	16.45*5
Second planet carrier	16.45*5
Second sun gear	16.45*25
Parallel gear	16.45*25
Parallel pinion	-16.45*92
Generator	-16.45*92

7.1.1 Model of Stage 1

For the stage 1 model, the torsional stiffness of the shafts, gear meshing stiffness and inertia of all components are the user-supplied parameters in the Parameter mode.

The drivetrain data are listed in Table 7.2 [49].

Table 7.2 Drivetrain Data

Name	Value
J_1-inertia of rotor (kg·m2)	$4.8 \cdot 10^6$
J_2-inertia of low speed of shaft (kg·m2)	2500
J_3-inertia of first planet carrier (kg·m2)	80
J_4-inertia of first planet gear (kg·m2)	5
J_5-inertia of first sun gear (kg·m2)	10
J_6-inertia of first intermediate shaft (kg·m2)	100
J_7-inertia of second planet carrier (kg·m2)	65
J_8-inertia of second planet gear (kg·m2)	3
J_9-inertia of second sun gear (kg·m2)	8
J_{10}-inertia of second intermediate shaft (kg·m2)	50
J_{11}-inertia of intermediate speed gear (kg·m2)	18
J_{12}-inertia of high speed gear (kg·m2)	1
J_{13}-inertia of high speed shaft (kg·m2)	15
J_{14}-inertia of generator (kg·m2)	200
K_1-stiffness of low speed shaft (Nm/degree)	$1.79 \cdot 10^6$
K_2-stiffness of first planetary gear meshing (N/m)	$1.2 \cdot 10^8$
K_3-stiffness of first intermediate shaft (Nm/degree)	488000
K_4-stiffness of second planetary gear meshing (N/m)	$1.0 \cdot 10^8$
K_5-stiffness of second intermediate shaft (Nm/degree)	360000
K_6-stiffness of parallel gear meshing (N/m)	$2.0 \cdot 10^7$
K_7-stiffness of high speed shaft (Nm/degree)	42000
r_{1r}-first ring gear size (mm)	440
r_{1s}-first sun gear size (mm)	110

r_{2r}-first ring gear size (mm)	320
r_{2s}-first sun gear size (mm)	80
r_1-first parallel gear working pitch radius (mm)	184
r_2-second parallel gear working pitch radius (mm)	50
i-total gear ratio	1:92

When the user selects Simulation mode, the Linear analysis mode button 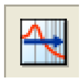 is enabled. Then select various components in the system. A new field is appended in the fourth column called Status. There are three items for a state variable in the menu: Free State, Fixed State and State Observer. State Observer is a free state that happens also to be an observer variable. In this report, change the status of the rotary speed of some variables as state observer. Click the LA Status, the dialog box is shown as in Figure 7.2. Be sure there are no fixed states and no control variables. It is also a necessary step that set linearization time, which could be enter in LA times.

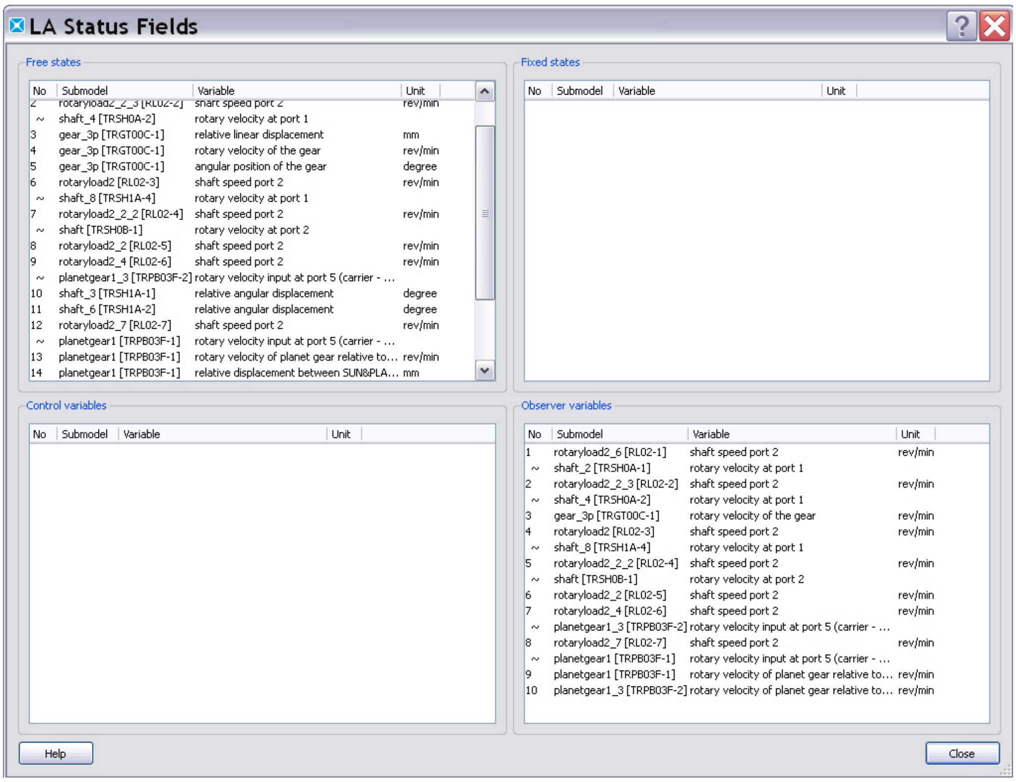

Figure 7.2 LA Status

After the simulation is done, click on the Eigenvalues Modal shapes button  to produce the Linear Analysis – Eigenvalues dialog box. The eigenvalues and the modal shapes of the drivetrain are obtained readily by means of Linear analysis. The natural frequencies in Hz are 0.50, 14.56, 36.10, 48.31, 87.24, 136.21, 153.99, 170.77, and 183.45. Compared with the natural frequencies in the reference paper[23], the number of eigen frequencies is small. This is partly because of the complexity of the drivetrain in the [23] is more complicate than this model, such as the bending of the blade, the tower flexibility are modeled.

First, the magnitude modal shape is plotted. In the gearbox, when comparing rotary mass velocities the gear ratio must be indicated. Therefore, the Magnitude factor is modified to facilitate the comparison, as in Figure 7.4. Modal shapes plotting magnitude at frequency 0.50 Hz are presented in Figure 7.5.

Another possibility is to use modal shapes plotting energy since the square of rotary velocity is proportional to energy and the constant of proportionality is the inertia which is already known. So energy modal shapes are introduced here in order to demonstrate each observer corresponding to the natural frequency. I,R,C factor in energies modal shape is modified in Figure 7.6. The energy modal shape at 0.50 Hz could also be plotted as seen in Figure 7.7.

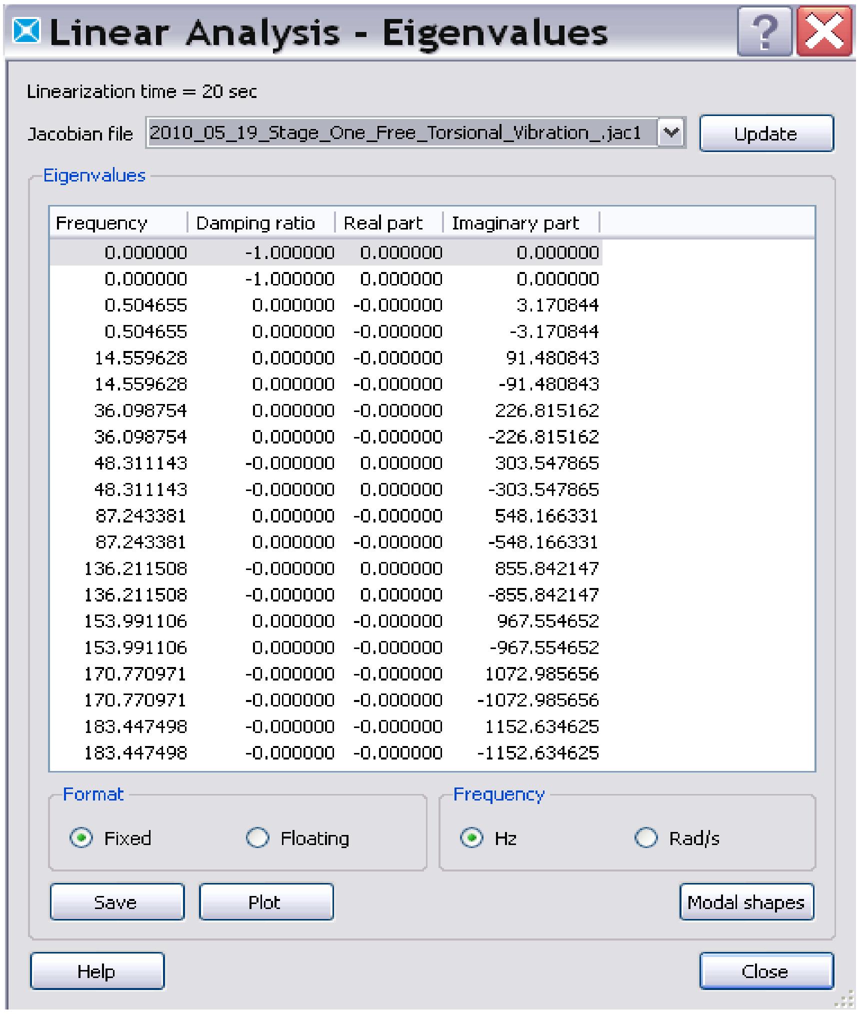

Figure 7.3 Eigenvalues of free torsional vibration for Stage 1

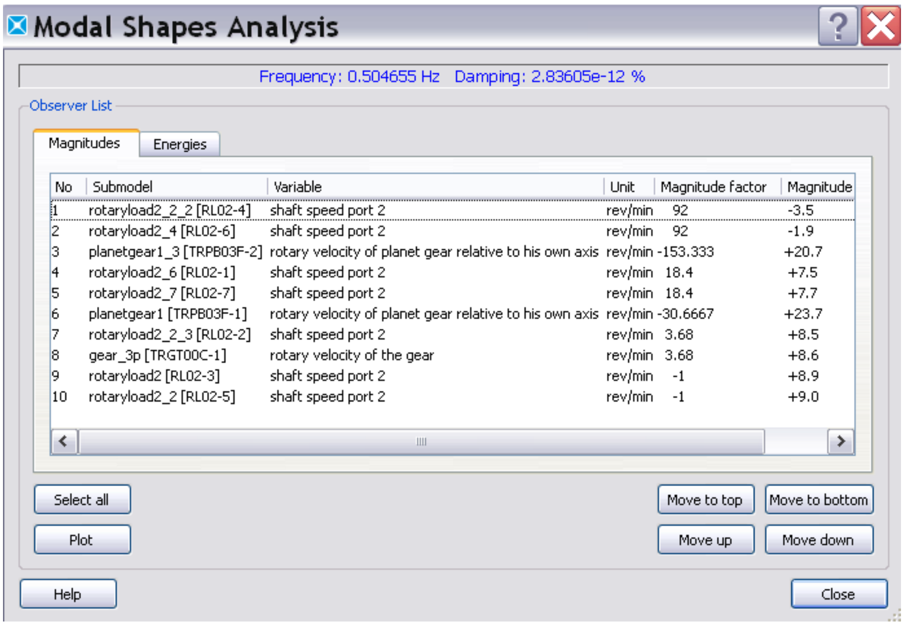

Figure 7.4 Magnitude factors of modal shapes

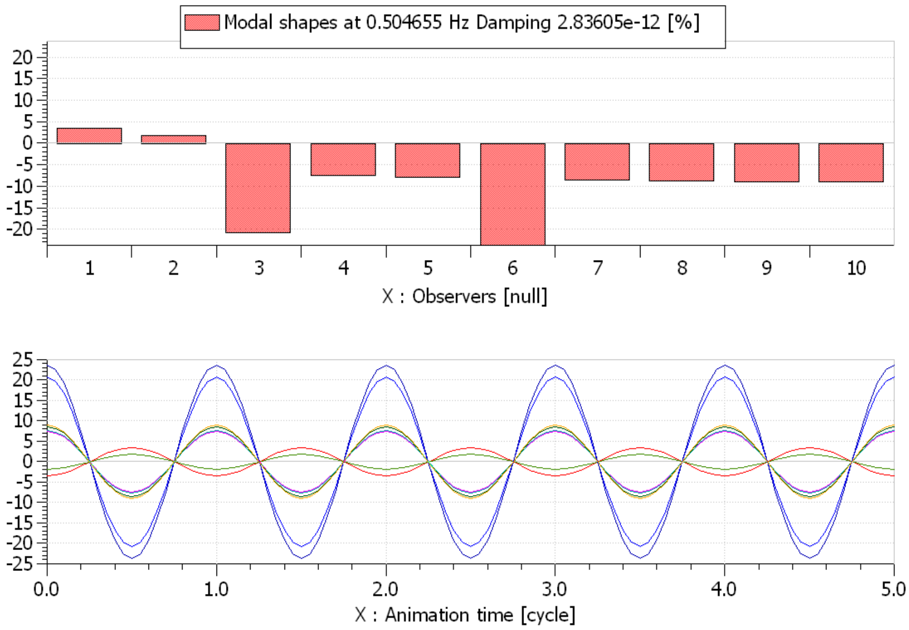

Figure 7.5 Magnitudes modal shape at frequency 0.50 Hz

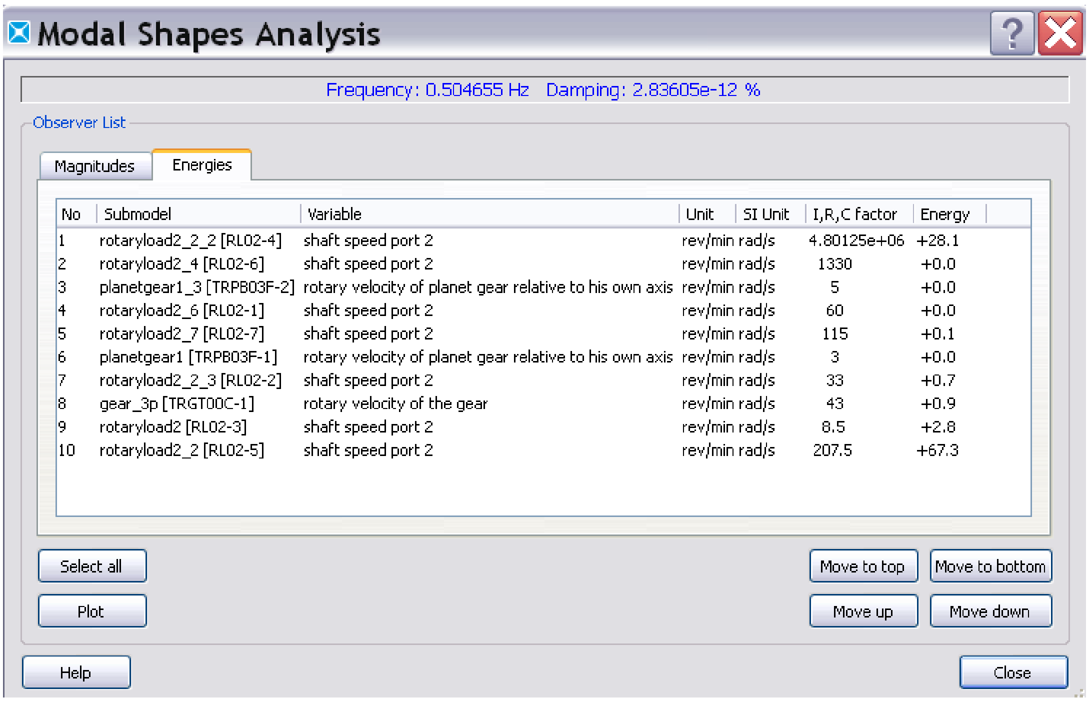

Figure 7.6 Energies factors of modal shape

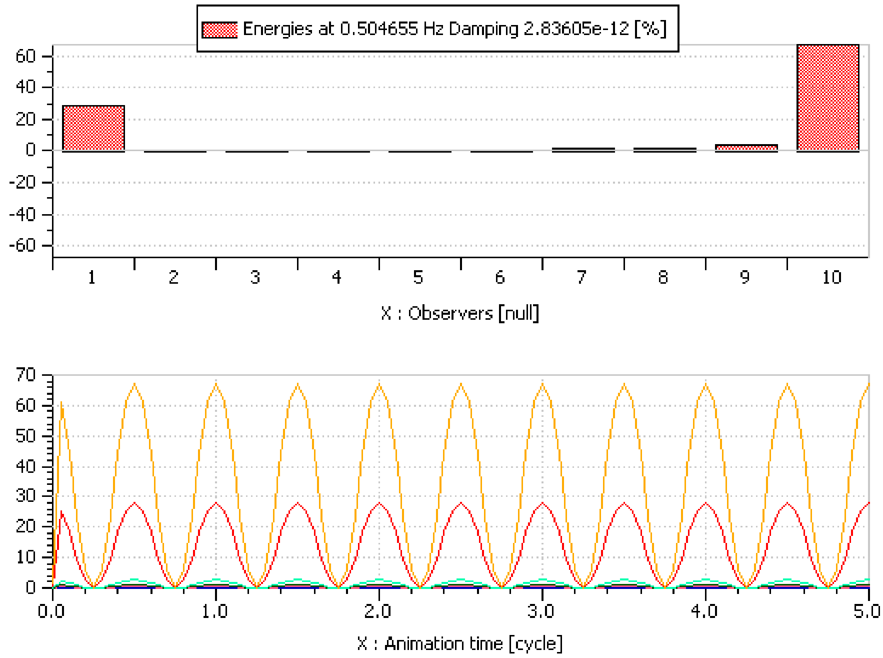

Figure 7.7 Energies modal shape at frequency 0.5 Hz

7.1.2 Model of Stage 2

Compared with the Stage 1, the Stage 2 system adds the torsional damping of shaft, Hertz stiffness, contacting damping of gear stages and backlash. Other material parameters are the same as previous model. The drivetrain model configuration use the Stage 1 concept, while in Parameter mode, there are some additional parameter to be entered.

Table 7.3 Added Data for the drivetrain

Name	Value
C_1-damping of low speed shaft (Nm/(rev/min))	25000
C_2-damping of first intermediate shaft (Nm/(rev/min))	20000
C_3-damping of second intermediate shaft (Nm/(rev/min))	15000
C_4-damping of high speed shaft (Nm/(rev/min))	12000
C_5-contact damping of first planetary (Nm/(m/s))	25000
C_6-contact damping of second planetary (Nm/(m/s))	20000
C_7-contact damping of parallel gear stage (Nm/(m/s))	15000
tot_1-total clearance of first planetary (mm)	3
lim_1-limit penetration of first planetary (mm)	0.03
tot_2-total clearance of second planetary (mm)	2
lim_2-limit penetration of second planetary (mm)	0.02
tot_3-total clearance of first planetary (mm)	1.5
lim_3-limit penetration of first planetary (mm)	0.015
modulus of elasticity	$2.1 \cdot 10^{11}$
Poisson's ratio	0.29

Do the same procedure for this model, and choose the same state observer. Click on the Eigenvalues Modal shapes button  to produce the Linear analysis. The natural frequencies in Hz of this model are 3.35, 23.37, 24.05, 44.20, 746.87, 1197.63, and 2230.17. Compared with the natural frequencies in the previous model, the number of Eigen frequencies is smaller but the highest frequency is larger than that. This is partly due to the introduction of the damping coefficient, Hertz stiffness and the backlash between the gears. Also, the mode shapes of magnitudes and energies are created.

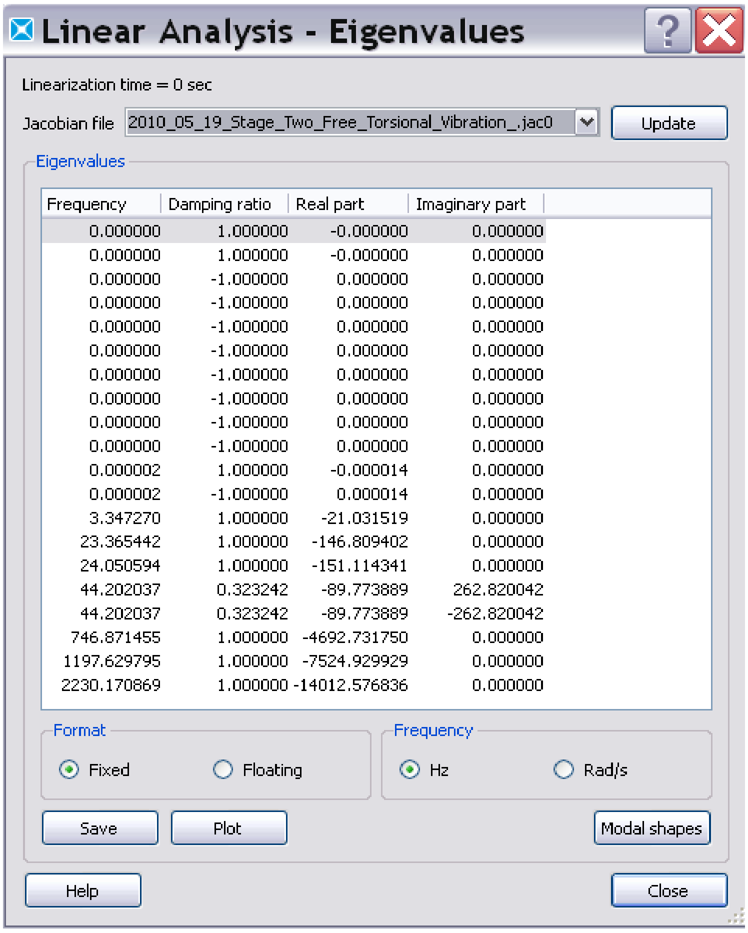

Linear Analysis - Eigenvalues

Linearization time = 0 sec

Jacobian file 2010_05_19_Stage_Two_Free_Torsional_Vibration_.jac0 Update

Eigenvalues

Frequency	Damping ratio	Real part	Imaginary part
0.000000	1.000000	-0.000000	0.000000
0.000000	1.000000	-0.000000	0.000000
0.000000	-1.000000	0.000000	0.000000
0.000000	-1.000000	0.000000	0.000000
0.000000	-1.000000	0.000000	0.000000
0.000000	-1.000000	0.000000	0.000000
0.000000	-1.000000	0.000000	0.000000
0.000000	-1.000000	0.000000	0.000000
0.000000	-1.000000	0.000000	0.000000
0.000000	-1.000000	0.000000	0.000000
0.000002	1.000000	-0.000014	0.000000
0.000002	-1.000000	0.000014	0.000000
3.347270	1.000000	-21.031519	0.000000
23.365442	1.000000	-146.809402	0.000000
24.050594	1.000000	-151.114341	0.000000
44.202037	0.323242	-89.773889	262.820042
44.202037	0.323242	-89.773889	-262.820042
746.871455	1.000000	-4692.731750	0.000000
1197.629795	1.000000	-7524.929929	0.000000
2230.170869	1.000000	-14012.576836	0.000000

Format: Fixed / Floating — Frequency: Hz / Rad/s

Save Plot Modal shapes

Help Close

Figure 7.8 Eigenvalues of free torsional vibration for Stage 2

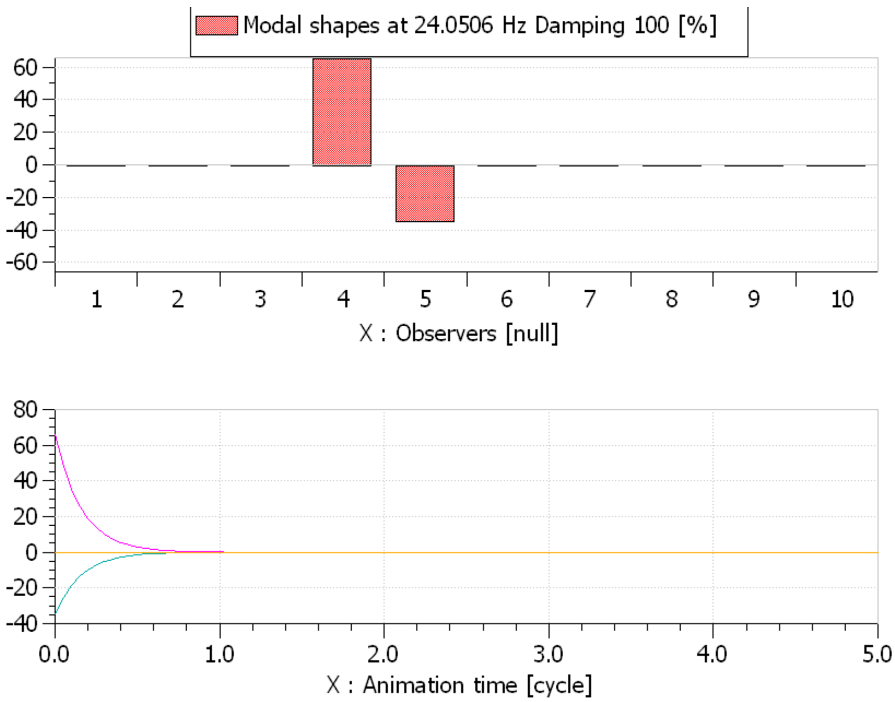

Figure 7.9 Magnitudes modal shape at frequency 24.05 Hz

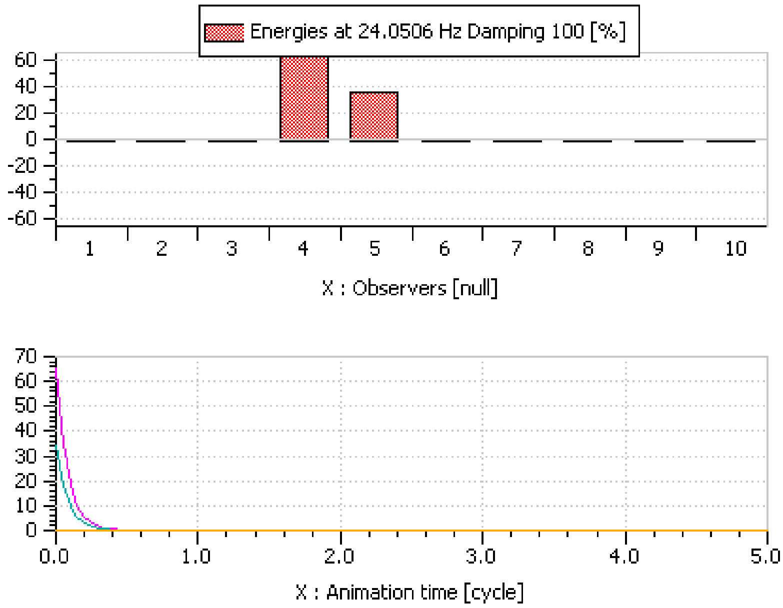

Figure 7.10 Energies modal shape at frequency 24.05 Hz

Introducing the Hertz stiffness, it is interesting to see the contact stiffness between the gear teeth. See the Figure 7.11. Backlash influences the local force between the gear wheels, especially the interval when there is no contact between the teeth. See the Figure 7.12.

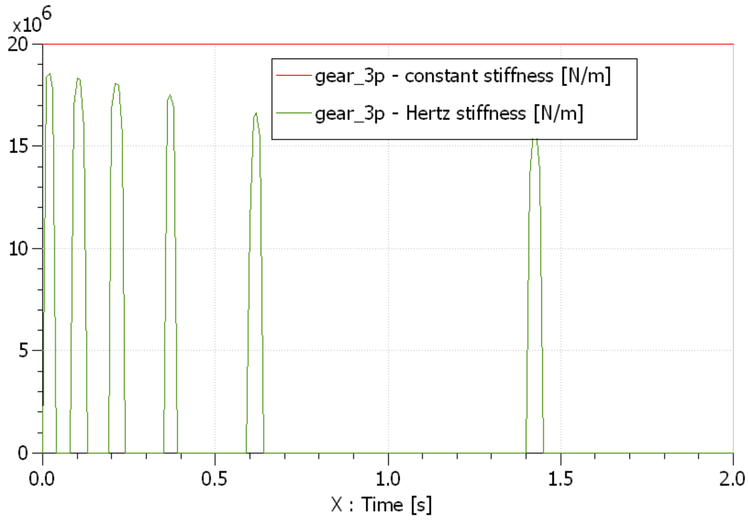

Figure 7.11 Comparison contact stiffness between the models of Stage 1 & 2

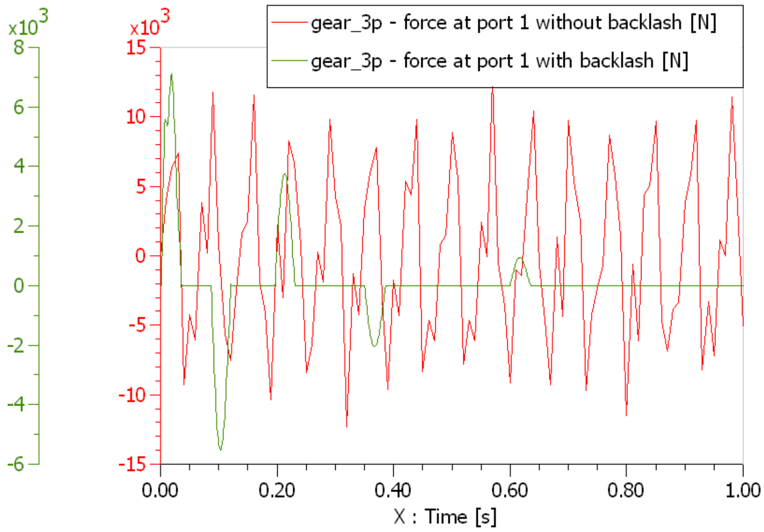

Figure 7.12 Comparison contact force of parallel gear stage between the models of Stage 1 & 2

7.2 Transient vibration dynamics

The models used in this section consist of the gearbox, aerodynamic torque and the generator torque. The drivetrain is possible to stand with the harsh transient conditions during normal operations due to the gusts, start-up and shut-down operations. In addition, it may also experience severe loads because of the generator or electrical network faults [5].

The accurate modeling of transient case demands a complete model of the wind turbine, including the aerodynamics and generator. Since the detail models for them are not available, the approaches discussed in Chapter 5 are used here for the torque excitation. The analytical approximation introduced in Section 5.1.2 and the ways for the electromagnetic torque in Section 5.2 are applied for this model. It is sufficient enough for the simulation of the drivetrain.

The transient load case chosen in this report is a sudden torque variation at the generator side with high amplitude, which is also presented in the report, [50]. This behavior has some reasons, for example transient due to lightning, electrostatic discharges, voltage dips resulting from the short circuits [51]. In this report, the torque transient occurs during the normal operation of wind turbine. It implies that the generator torque is almost constant as shown in Figure 7.12(a). Firstly, the simulation is done for this reference torque source. Then there is a sudden torque variation takes place at t=50s, which the shape and duration may differ largely from the electrical fault. Nevertheless, the signal for the transient load is enough for the dynamic analysis of the drivetrain. As seen in Figure 7.12(b), a damped sinusoidal source with a frequency 20 Hz. It lasts 100ms and has a highest magnitude of 12 kNm. This is a type of generator torque variation during a short circuit of a DFIG described in references [23, 52].

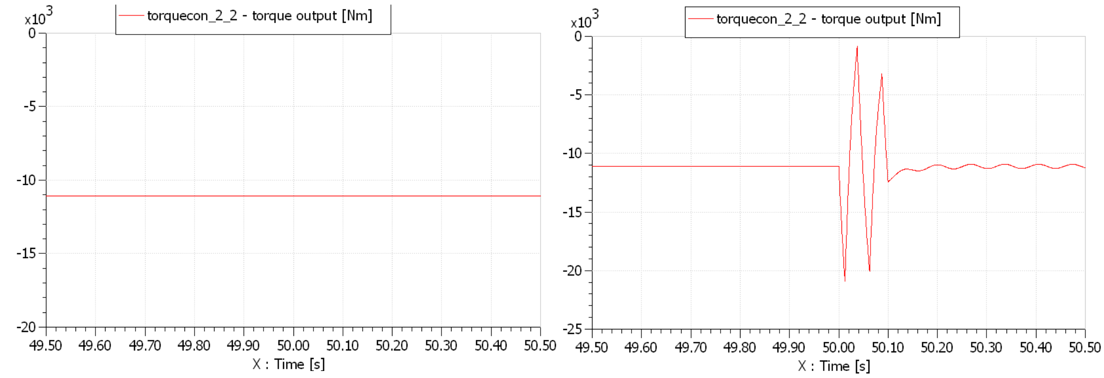

(a) the normal operation load case (b) a grid disturbance load case

Figure 7.12 Generator torque used in the simulation

7.2.1 Model of Stage 1

The drivetrain would consider the aerodynamics that is a steady state load case and the transient generator load case. The gearbox of Stage 1 is utilized to do analysis first; the following figure is the whole wind turbine model for the transient load case.

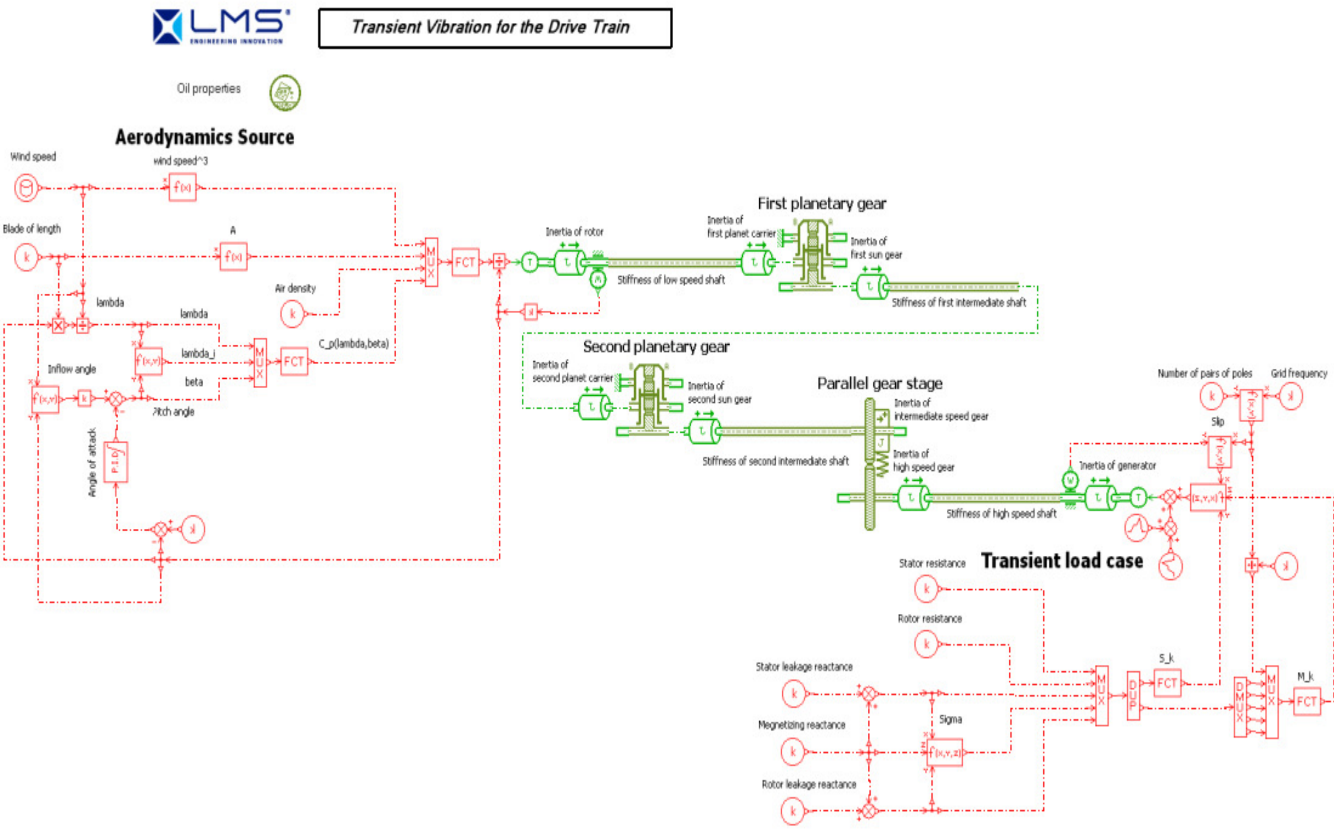

Figure 7.13 Wind turbine model with the transient load

Table 7.4 Rotor Characteristics

Name	Value
N-number of blades	3
D-rotor diameter (m)	80
V-nominal wind speed (m/s)	15.9
ω-nominal revolutions (rpm)	16.45
ρ-air density (kg/m3)	1.22

Table 7.5 Three-Phase Doubly Fed Induction Generator Data

Name	Value
R1-stator resistance (Ω)	0.001164
R_2'-rotor resistance (Ω)	0.00131
X_h-magnetizing reactance (Ω)	0.941
$X_{1\sigma}$-stator leakage reactance (Ω)	0.022
$X_{2\sigma}'$-rotor leakage reactance (Ω)	0.0237
U-voltage (V)	680
f-grid frequency (Hz)	50
p-number of pairs of poles	2

The above two tables are the rotor and the generator characteristics corresponding to the gearbox used in previous models. All the data are based on the description in reference [49, 53] of the wind turbine parameters.

Before jumping into the analysis of the influence due to transient load, it is necessary to look at the normal operation condition of wind turbine model. In the model, all the damping coefficients of mechanical components are ignored. There are two reasons for this: It is widely recognized that the rate of free decay of turbine-generator torsional oscillations following removal of all stimuli (forcing functions) is very small, which comparison to that of bending vibration, but this radial motion is practically nonexistent for torsional vibration [29]; Accurate values for the damping coefficients are usually difficult to obtain [54].

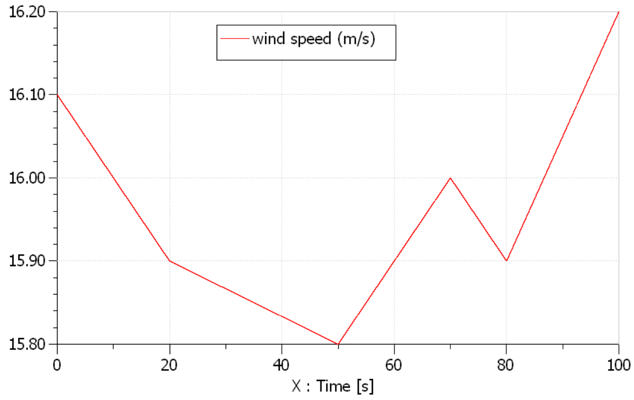

Figure 7.14 Wind speed versus time

As mentioned before, the wind speed is at nominal condition, so the speed varies within a small range of 15.9 m/s.

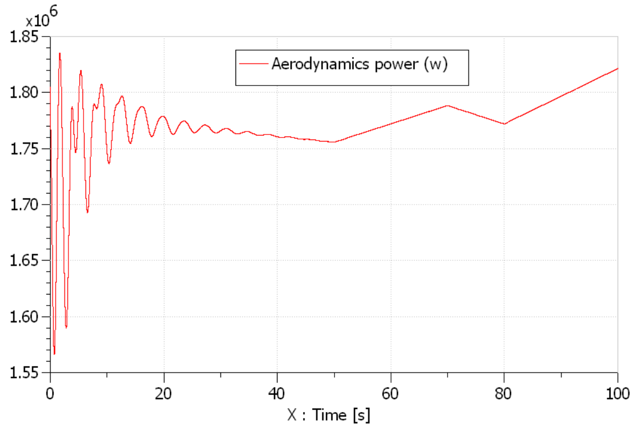

Figure 7.15 Aerodynamic power versus time

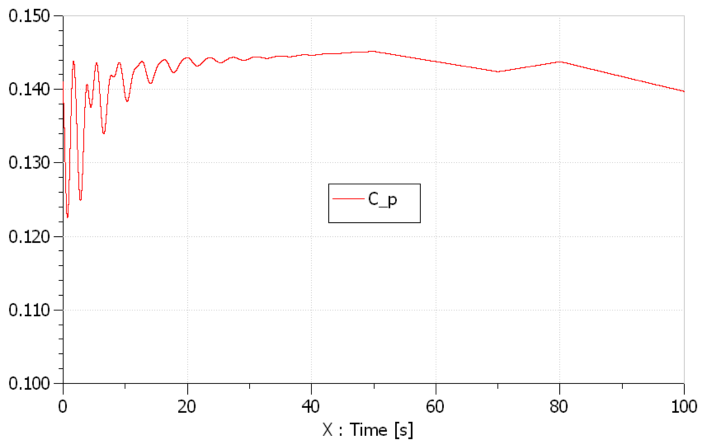

Figure 7.16 Power coefficients versus time

The rated power of corresponding wind turbine in reality is around 2 MW, while Figure 7.15 shows that the maximum is about 1.8 MW, which is lower than the rated power of wind turbine that this report refers to. Figure 7.16 partly explains why the output power from the rotor hub can't arrive at the maximum due to the low value of power coefficient. The power coefficient is determined by the analytical approximation where the P.I.D controller is a core control theory for the calculation the desired angle of attack. As a result, the pitch angle could be obtained by inflow angle minus the angle of attack from P.I.D controller. However, in reality, the control part of wind turbine for pitch angle is much more complicated than that in this report. Actually, the simulation results of this model built in AMESim is sufficient to analyze the transient dynamics of the drivetrain.

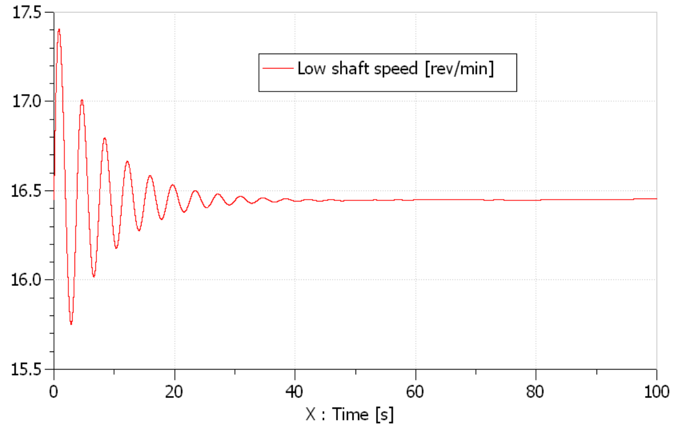

Figure 7.17 Revolution of main shaft versus time

The nominal revolution in the drivetrain model is 16.45 rpm; while Figure 5.13 shows the steady-state rotating speed of the main shaft is almost the same as the setting desired speed. It means that the P.I.D control in this model works well.

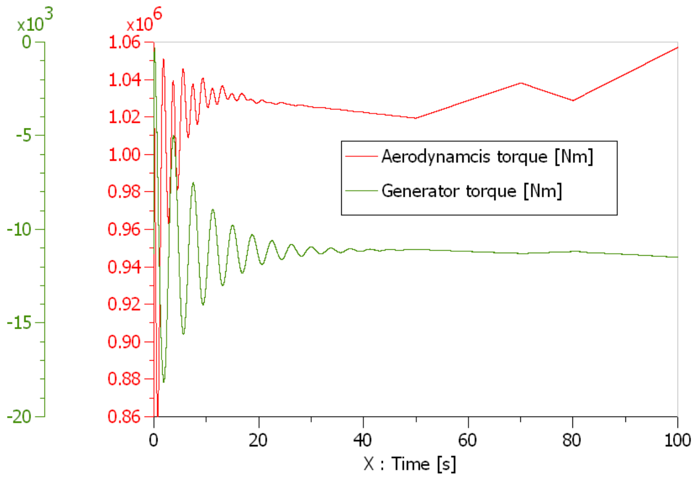

Figure 7.18 Aerodynamic & Generator torques versus time

The above diagram just verifies the relation between the aerodynamic torque and the generator torque, which is discussed in detail in Section 6.2.3. As shown in the figure, the value of the rotor hub torque is roughly 92 times higher than that of the electromagnetic torque, while the signs of them are just opposite.

To sum up the above arguments, the multibody model of dynamics of drivetrain, taking into account the aerodynamic model and the generator model, is accurate enough to demonstrate the torque transmission from the rotor hub through the gearbox to the generator, which is the critical and also fundamental step in order to update the existing model.

The aerodynamic and generator modeling approaches in this 1-D dynamic simulation model are based on the assumption that the wind turbine operates at the nominal condition, in which the wind speed is nominal speed, the nominal revolution of the main shaft and the rated power of the rotor hub. The run simulation time is duration of 100s, whereas at the beginning of the simulation, the system is not stable until at the time of 40s. Therefore, the simulation results that is valuable enough to study starts at t = 40 sec.

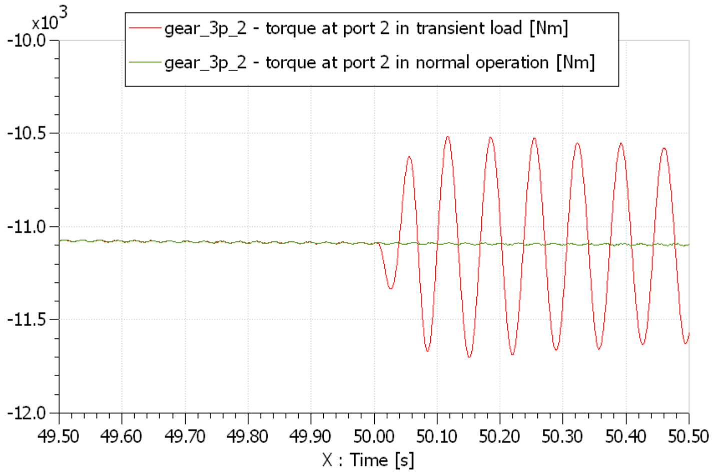

Figure 7.19 Torque at the pinion of the parallel stage

The Figure 7.19 shows the level comparison of the torque that acts on the high speed pinion of the simulation for the two generator load cases. The torque transient in the generator due to the grid short circuit disturbance produces the load variation in the pinion. The amplitude of the pinion peak torque is around 0.5 kNm, which is twentieth of the generator torque at the normal mode. This absolute value is further needed to be verified by the experimental data. The damping in the drivetrain and the coupling type also affect the level of the torque variation of the pinion.

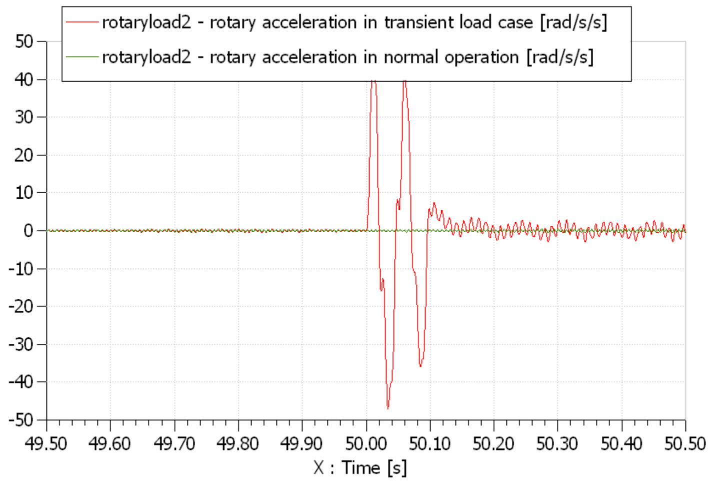

Figure 7.20 Rotary acceleration of the pinion of parallel stage

The network disturbance resulting in the sudden torque peak in the generator accelerates the rotating speed of the pinion quickly and abruptly. The magnitude of the acceleration of the pinion at the parallel stage arrives at the 40 rad/s^2, which is roughly 40 times higher than the value at the normal mode of the wind turbine.

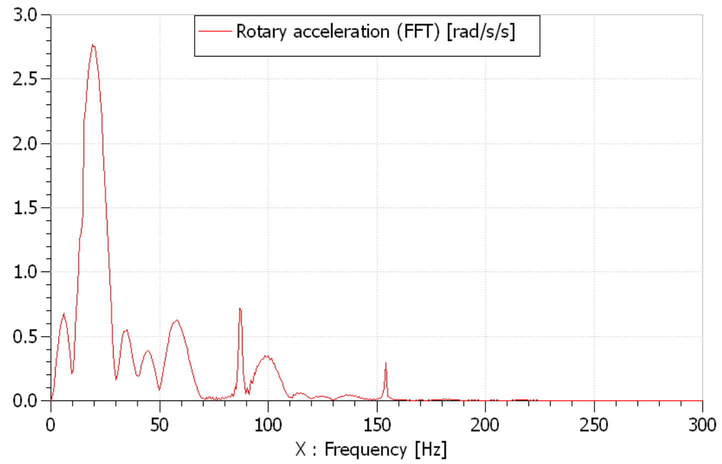

Figure 7.21 The frequency of the rotating acceleration of pinion at transient load case

7.2.2 Model of Stage 2

The model is the same as the previous model of Stage 1 for the transient load case. This model at Stage 2 would include the damping coefficient and Hertz stiffness, backlash. Therefore, it is interesting to see what happens to the pinion at Stage 2 compared with the result at Stage 1 under the grid disturbance condition.

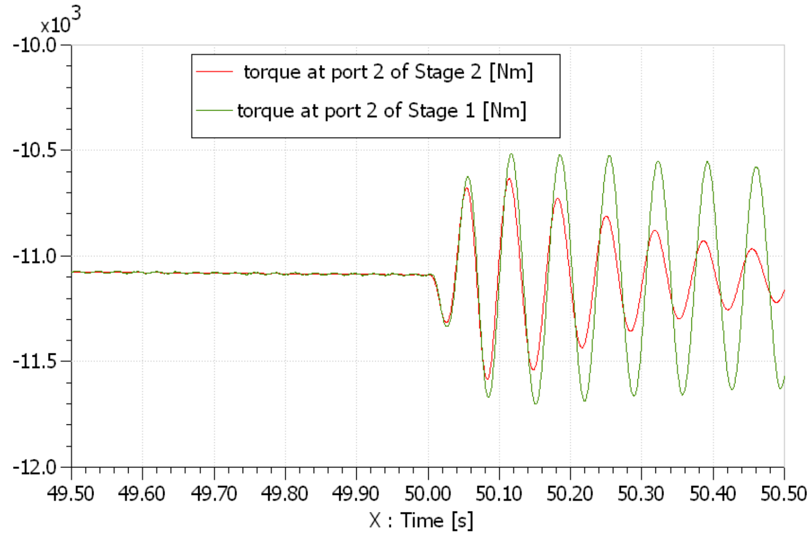

Figure 7.22 Torque at the pinion of the parallel gear stage

The Figure 7.22 shows the level comparison of the torque that acts on the high speed pinion of the simulation for two stages' models. The levels of the amplitudes for both models are at the same order. What is more important, the red curve indicates the rate of decay of wind turbine torsional oscillations following has an obvious effect on the torque variation, while the green line decays really slowly. The experimental validation of the numerical models is also demanded in order to proof the simulation results.

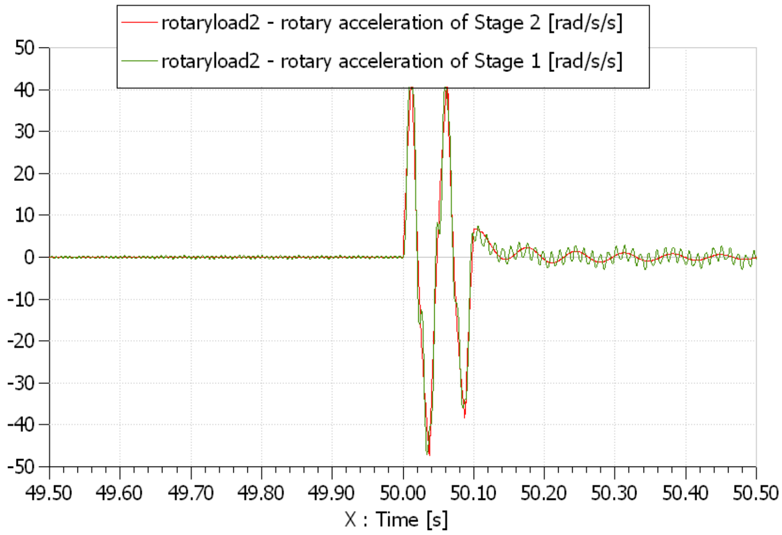

Figure 7.23 Rotary acceleration of the pinion of parallel gear stage

The result of the rotating acceleration is similar to that of Stage 1. The magnitude of acceleration still arrives at the 40 rad/s^2, but the oscillation of the rotary acceleration decreases a lot comparison with the model without damping.

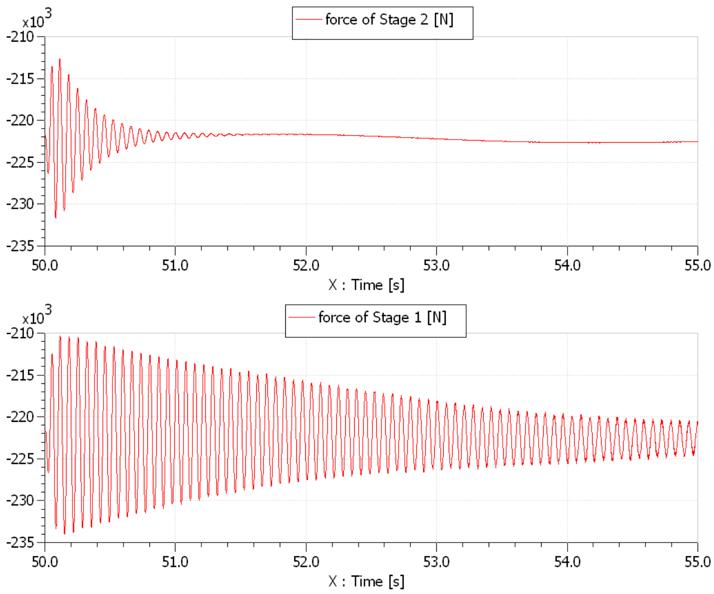

Figure 7.24 The force between the gear teeth of parallel gear stage

The damping phenomenon happens to the contact force between the gear teeth at the parallel gear stage. The vibration of Stage 2 is damped rapidly and also the highest amplitude is a bit smaller than the force of Stage 1. This could be demonstrated better in Figure 7.25. The Fast Fourier Transform is employed in the contact force figures of the parallel gear stage in the time history between the times of 50s and 55s. It shows that the local modes in the parallel stage at 14.6 Hz. The value of Stage 1 indicates there is considerable force amplification. Whereas the damping effect of Stage 2 has a significant influence in the amplitude of the gear teeth force.

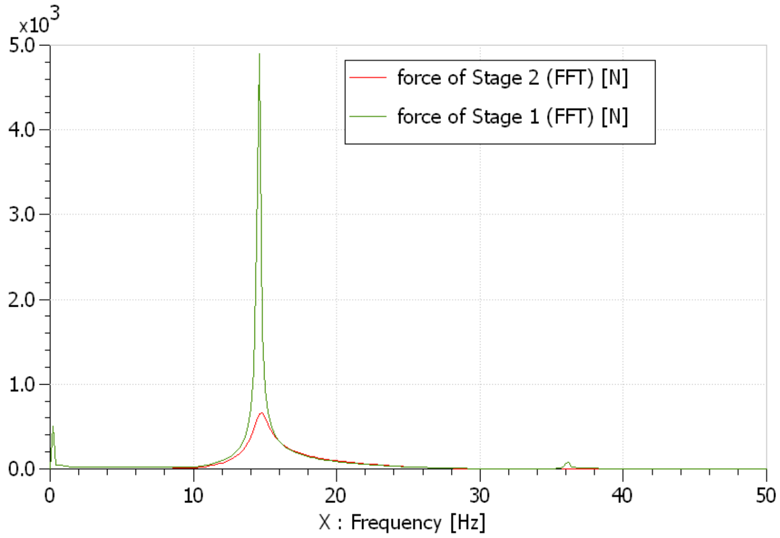

Figure 7.25 The force frequency between the gear teeth of parallel gear stage

7.3 Steady state vibration

In this part, the focus is put on the power loss calculation due to the bearing loss, which is talked about in the Section 6.3.4. The aim of the simulation is to characterize the losses from the bearing at the normal operation of the wind turbine. Therefore, the input torques from the aerodynamics and generator are stable during the simulation in order to calculate the power losses.

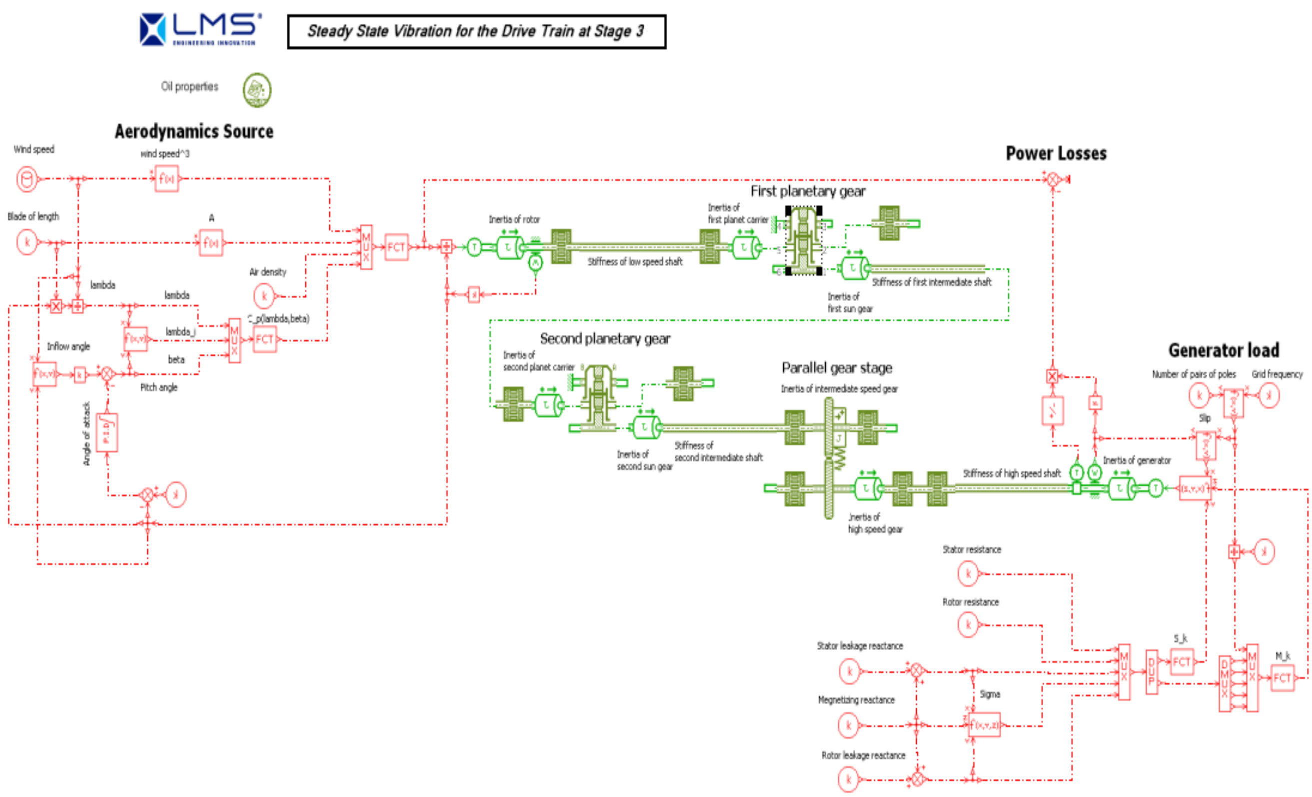

Figure 7.26 The sketch of the power loss calculation model of Stage 3

As seen from the Figure 7.27, the bearing configuration model resulting in the power loss could simply simulate the power loss. It is a non-ignored number compared to the total mechanical power from the wind, which account for 3% in total. In addition, in this model, the bearing model only considers the constant load for the bearing and the losses only come from hydraulic. The losses from the load and preload are also not included here because the axial and radial load of bearing is unknown and varying all the time. What's more important is that the gear losses are also a critical power loss source, such as slipping losses and rolling losses in gears contacts and paddling losses on gears teeth. Due to the limit of the submodel of planetary gear in AMESim, the power loss of gear losses can't be taken into account in this report. The power losses from gear and bearing due to load and preload are also essential factors and should be taken into account in the future works.

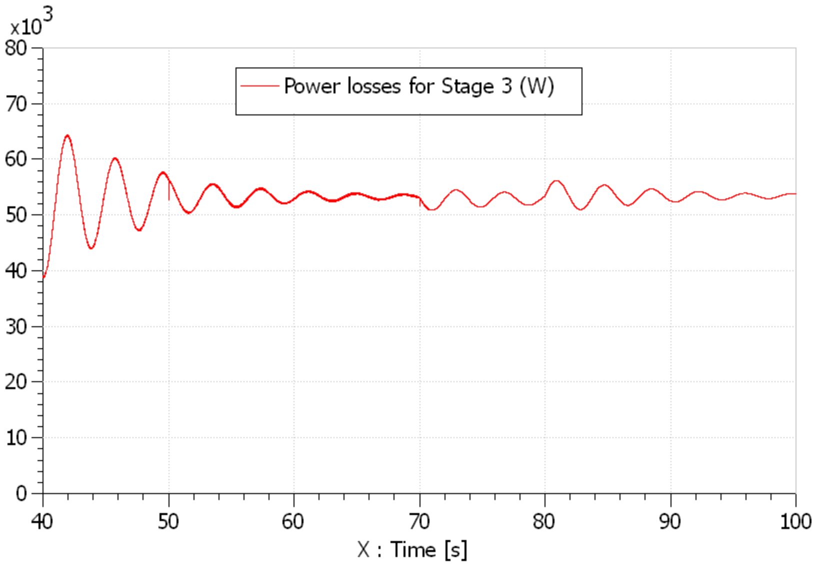

Figure 7.27   Power losses due to bearing

8 Conclusion and suggestions for future work

8.1 Conclusions

The main purpose of this work is to learn about the dynamic behavior of the drivetrain in the wind power. The report starts from the statement that there is a high downtime per failure of drivetrain per year among the different components of the wind turbine. Misalignment is discovered and considered as one of the main contributors to the failure of the gearbox [3]. Therefore, to investigate the internal drivetrain components behavior is an interesting and meaningful work.

The fundamentals of the components used in a wind turbine are presented. Various drivetrain concepts existing in the wind industry are presented. In particular, the typical drivetrain configurations that are commercially wide-popular are intended to be reviewed and applied in the dynamic model for the project. The typical concept is called baseline modular wind turbine with drivetrain. It is a three stage gearbox with two spur planetary gear stages following by one spur parallel gear stage. The multi-body simulation techniques of different levels of complexity, used within the scope of the project are described in detail. For early design stages, a purely torsional MBS proved to a suitable solution and is selected to demonstrate the dynamic behavior of wind turbine gearbox.

The methods how to simulation the aerodynamic torque at the normal rating operation condition and the typical $Klo\beta's$ equation for the asynchronous machine are discussed clearly and the complete wind turbine employs them to build the dynamic model. In AMESim, there are extensive dedicated libraries ranging from the mechanical, electric, hydraulic, pneumatic and thermal components. Even the complicated planetary component is a ready-to-use physical submodel, AMESim actually convenient to build the 1-D multi-domain system and save enormous amounts of time by dedicated libraries.

1-D mechanical torsional vibration models in AMESim are divided into three levels of complexity including the rotor blade and the generator components in order to investigate the dynamic behavior of drivetrain. The model at Stage 1 is one simplest torsional system of drivetrain with the only flexibilities existing in the rotating shafts and the gear meshing. Stage 2 takes the advantage of AMESim consisting of the damping coefficient of shafts and gear contact, backlash of the gear stages and also more realistic gear contact stiffness-Hertz stiffness. At the last stage, the model is based on the previous model, further introducing the bearing loss. The simulation is divided into three ways to demonstrate the dynamic characteristics of the gearbox. The first section deals with gearbox model without the extension in order to do free torsional vibration analysis. The torsional multibody methodology facilities the determination of both eigenvalues and mode shapes of the models at Stage 1 and Stage 2, so these are required to be presented to check the differences due to the complexity of the models. The contact stiffness of gear stages varies with contacting assumption. Then the second section extends the model with extra components at the rotor and generator sides for transient vibration dynamics. The transient conditions may come from the short circuits in the electrical network, gusts resulting in severe load case and reverse torque due to emergency stop etc. The torque variation due to short circuit is applied in the dynamic model in order to yield the insight in the drivetrain behavior and much detailed information. The transient load yields a torque peak on the pinion of the high speed stage, high rotational acceleration levels for the pinion also. Finally, the steady state vibration analysis is focusing on the calculation of power losses due to the influence of the bearing loss. The simulation result indicates that the power loss accounts for 3% of the total mechanical power obtained from the wind.

8.2 Future work

The thesis indicates the need for employing more advanced models in the simulation of drivetrain loads in a wind turbine. It is a pre-study of dynamics of drivetrain and the starting point of the research. Subsequently, it requires much more work in order to decrease the failure rate of drivetrain and obtain more availability of the wind turbine. The recommendations presented here is a further improvement of the model representation of drivetrain in order to improve the quality of load simulations. Several suggestions to further improve and extend the present job are listed following:

1. At the beginning of the report, it refers to the significance of misalignment to the overhaul of gearbox components. So the model requires being updated to take into account of the misalignment. There are possible locations where misalignments may occur in the drivetrain, the bearing and bearing housing, the gear meshing etc. It demands the introduction of more components flexibilities in the model, such as housing components, gearbox support, nacelle and tower.
2. The model developed in this report is 1-D dynamic model, which is the simplest model with one degree of freedom per drivetrain component only suitable for investigation of torsional vibrations in the drivetrain. Therefore, it is difficulty in simulating the internal loads and stress inside the drivetrain. In this point of view, it is necessary to apply more degrees of freedom in the drivetrain model and more advanced modeling method, like a rigid 6 DOFs MBS even a flexible MBS including a reduced FE submodels for critical components. This could be done a combination with other multi-body simulation software, like LMS Virtual.Lab, ADMAS etc.
3. All the simulation results presented in this report should be verified by experimental test. In other words, the numerical models are validated by checking them with the test results from future measurement of wind turbine prototype.
4. The realistic and accurate parameter values of components can help in making the dynamic model closed to the reality and also increase the reliability and efficiency of model validation. Especially the determination of stiffness values for shafts and gears is complicated but necessary for the realistic model.
5. In the transient case, the representation of short circuit in the electrical grid is a simple simulation. Since the accuracy of transient load condition depends highly on accuracy of occurrence, it is recommended to build the more detailed generator and electrical grid model in AMESim or Simulink. Then the appropriate description of excitations due to transient cases is possible to achieve.

9 References

1. *Wind Energy THE FACTS*. Architecture of a Modern Wind Turbine; Available from: <http://www.wind-energy-the-facts.org/en/part-i-technology/chapter-3-wind-turbine-technology/evolution-of-commercial-wind-turbine-technology/architecture-of-a-modern-wind-turbine.html>.

2. *Design process at fault -- Gearbox research*, in *Windpower Monthly Magazine*. September 2007.

3. Johan Ribrant, Bertling L, *Survey of failures in wind power systems with focus on Swedish wind power plants during 1997-2005.* IEEE Trans. Energy Conversion, 2007.

4. F. Spinato, P.J. Tavner, G.J.W. van Bussel and E.Koutoulakos, *Reliability of wind turbine subassemblies.* IET Renewable Power Generation, 2008.

5. Zhang Zhiwei, Nawazish Al-Zaidi, Christopher Halse and Ashley R. Crowther, *The Effect of Transient Loading on the Stresses of Wind Turbine Drivetrain Components.* 2009.

6. Coultate John, Daniel Edwards, Zhiwei Zhang, Christopher Halse, Ashley R. Crowther, *An Investigation into the Effect of Lateral and Axial Aerodynamic Loads on Wind Turbine Gearbox Reliability.* 2009.

7. B. K. N. Rao (ed.). 1996, Oxford: Elsevier Science Ltd.

8. W. Musial and S. Butterfield, *Improving Wind Turbine Gearbox Reliability* in *2007 European Wind Energy Conference*. May 2007: Milan, Italy

9. G. Bywaters, V. John, J. Lynch, P. Mattila, G. Norton, J. Stowell, M. Salata, O. Labath, A. Chertok and D. Hablanian, *Northern Power Systems WindPACT Drive Train Alternative Design Study Report*. 2004, National Renewable Energy Laboratory.

10. *Alternative Energy news and information resources about renewable energy technologies*. Available from: http://www.alternative-energy-news.info/technology/wind-power/wind-turbines/.

11. *Get Off The Grid---Wind Power Saving*. Available from: http://www.windpowersavings.com/how-do-wind-turbines-work/14/.

12. R. Gasch, Twele, J. , *Wind Power Plants Fundamentals: Design, Construction and Operation* 2002, Berlin Solarpraxis AG

13. F. Oyague, *Gearbox Modeling and Load Simulation of a Baseline 750-kW Wind Turbine Using State-of-the-Art Simulation Codes* February 2009, National Renewable Energy Laboratory.

14. *Voith - WinDrive*. Available from: http://www.voithturbo.com/wind-technology_operating-principle-in-detail.htm.

15. Prof. Dr.-Ing. Berthold and Dipl.-Ing. Tobias Schulze Schlecht, *Simulation of Drive Trains in Wind Turbines with SIMPACK*, in *SIMPACK User Meeting*. April 2003: Breisgau.

16. Nordex. Available from: http://www.nordex-online.com/en/nordex/downloads.html#c4161.

17. Misalignment. Available from: http://www.dliengineering.com/vibman/misalignment.htm.

18. John Piotrowski, *Shaft Alignment Handbook*. Second Edition ed. 1995, New York.

19. Michele Lucente, *Condition monitoring system in wind turbine gearbox*. 2008, Royal Institute of Technology: Stockholm.

20. Michael.R.Wilkinson, *Condition monitoring of wind turbine drive trains*, in *ICEM*. 2006: Crete, Greece. p. 441.

21. SKF. *SKF WindCon 3.0 online condition monitoring system*. Available from: www.skf.com.

22. P. Caselitz, J.Giebhardt, *Advanced maintenance and repair for offshore wind farms using fault prediction techniques*. 2002, ISET: Berlin.

23. Prof. Dr. Ir. D. and Prof. Dr. Ir. P. Sas Vandepitte, *Simulation of Dynamic Drive Train Loads in A Wind Turbine*. 2006.

24. J. Helsen, D. Vandepitte, W. Desmet, J. Peeters, S. Goris, F.Vanhollebeke, B. Marrant and W.Meeusen, *From Torsional Towards Flexible 6 DOF Models for Dynamic Analysis of Wind Turbine Gearboxes*. 2008, K.U.Leuven, Department of Mechanical Engineering.

25. Joris L. M. Peeters, Dirk Vandepitte and Paul Sas. *Analysis of Internal Drive Train Dynamics in a Wind Turbine*. 2005; Available from: www.interscience.wiley.com.

26. J. Helsen, G. Heirman, D. Vandepitte and W. Desmet, *The influence of flexibility within multibody modeling of multi-megawatt wind turbine gearboxes*. 2008, PROCEEDINGS OF ISMA: Heverlee, Belgium.

27. ANSI/AGMA 110.04-1980, *Nomenclature of Tooth Failure Modes* 1989.

28. F. Oyague, *Progressive Dynamical Drive Train Modeling as Part of NREL Gearbox Reliability Collaborative* in *WINDPOWER 2008 Conference and Exhibition* 2008: Houston, Texas

29. Duncan N.Walker, *Torsional Vibration of Turbo-Machinery*. 2003: McGraw-Hill.

30. Maurice L.Adams, *Rotating Machinery Vibration*. 2001, New York: Marcel Dekker, Inc.

31. Wikipedia. *Normal Mode*. 2010; Available from: http://en.wikipedia.org/wiki/Normal_mode.

32. Daniel J.Inman, *Engineering Vibration*. 1994: Prentice-Hall, Inc.

33. J.F. Manwell, J.G.Mcgowan and A.L.Rogers, *Wind energy explained*, ed. Second edition. 2009: A John Wiley and Sons, Ltd.

34. Tony Burton, David Sharpe, Nick Jenkins and Ervin Bossanyi, *Wind Energy Handbook*. 2001: John Wiley and Sons, Ltd.

35. M.Hansen, *Aerodynamics of Wind Turbines*. 2001: Earthscan Publications Ltd.

36. Anders Ahlstrom, *Aeroelastic simulation of wind turbine dynamics*, in *Department of Mechanics*. 2005, Royal Institute of Technology: Stockholm.

37. Abram Perdana, *Dynamic Models of Wind Turbines*, in *Department of Energy and Environment*. 2008, Chalmers University of Technology: Goteborg, Sweden.

38. S.Heier, *Grid Integration of Wind Energy Conversion Systems*. 1998: England: John Wiley & Sons.

39. Nordex. 2009; Available from: www.nordex.com.

40. Siegfried Heier, *Grid Integration of Wind Energy Conversion Systems*. 2006: John Wiley & Sons, Ltd.

41. Prof. Dr.-Ing. Berthold Schlecht, *Multibody-System-Simulation of Drive Trains of Wind Turbines*, in *Fifteh World Congress on Computational Mechanics*. 2002: Vienna, Austria.

42. Vladislav Akhmatov, *Induction Generators for Wind Power*. 2005: Multi-Science Publishing Company, Ltd.

43. Wikipedia. *LMS*. 2010; Available from: http://en.wikipedia.org/wiki/AMESim.

44. LMS. *LMS*. 2010; Available from: http://www.lmsintl.com/.

45. Bonus, *Bonus-Info Newsletter*. 1998.

46. AMEHelp, *AMESim demo help*. 2010.

47. ANSI/AGMA, *AGMA Standard 110.04*, in *Nomenclature of Tooth Failure Modes*. 1980.

48. Windpower Monthly Magazine. *The role of bearings in gearbox failure*. 2005; Available from: http://www.windpowermonthly.com/news/959698/role-bearings-gearbox-failure/?DC.

49. M.Todorov, *Analysis of Torsional Oscillation of the Drive Train in Horizontal-Axis Wind Turbine.* IEEE, 2009.

50. J.Peeters, *Structural analysis of a wind turbine and its drive train using the flexible multibody simulation technique.* 2006.

51. J.Soens, *Interaction between Electrical Grid Phenomena and the Wind Turbine's Behaviour.* 2004.

52. S.Seman, *Transient Analysis of Doubly Fed Wind Power Induction Generator Using Coupled Field-Circuit Model* in *Proceedings of the 16th International Conference on Electrical Machines*. 2004: Krakow, Poland.

53. T. Kooijman, *Aero-elastic modeling of the DOWEC 6MW pre-design in PHATAS*. 2003.

54. John M.Vance, *Rotordynamics of Turbomachinery*. 1988: John Wiley &Sons.